RESEARCH ARTICLE

WILEY

Graph-theoretical analysis of EEG functional connectivity during balance perturbation in traumatic brain injury: A pilot study

Vikram Shenoy Handiru[1,2] (iD) | Alaleh Alivar[1,2] | Armand Hoxha[1] | Soha Saleh[1,2] (iD) | Easter S. Suviseshamuthu[1,2] | Guang H. Yue[1,2] | Didier Allexandre[1,2]

[1]Center for Mobility and Rehabilitation Engineering Research, Kessler Foundation, West Orange, New Jersey

[2]Department of Physical Medicine and Rehabilitation, Rutgers University New Jersey Medical School, Newark, New Jersey

Correspondence
Vikram Shenoy Handiru, Center for Mobility and Rehabilitation Engineering Research, Kessler Foundation, West Orange, NJ.
Email: vshenoy@kesslerfoundation.org

Abstract

Traumatic brain injury (TBI) often results in balance impairment, increasing the risk of falls, and the chances of further injuries. However, the underlying neural mechanisms of postural control after TBI are not well understood. To this end, we conducted a pilot study to explore the neural mechanisms of unpredictable balance perturbations in 17 chronic TBI participants and 15 matched healthy controls (HC) using the EEG, MRI, and diffusion tensor imaging (DTI) data. As quantitative measures of the functional integration and segregation of the brain networks during the postural task, we computed the global graph-theoretic network measures (global efficiency and modularity) of brain functional connectivity derived from source-space EEG in different frequency bands. We observed that the TBI group showed a lower balance performance as measured by the center of pressure displacement during the task, and the Berg Balance Scale (BBS). They also showed reduced brain activation and connectivity during the balance task. Furthermore, the decrease in brain network segregation in alpha-band from baseline to task was smaller in TBI than HC. The DTI findings revealed widespread structural damage. In terms of the neural correlates, we observed a distinct role played by different frequency bands: theta-band modularity during the task was negatively correlated with the BBS in the TBI group; lower beta-band network connectivity was associated with the reduction in white matter structural integrity. Our future studies will focus on how postural training will modulate the functional brain networks in TBI.

KEYWORDS
balance perturbation, EEG source localization, functional connectivity, graph theory, postural control, traumatic brain injury

1 | INTRODUCTION

Traumatic brain injury (TBI) is a significant medical and health problem in the United States, with an estimated 2.8 million people sustaining a TBI every year (Taylor, Bell, Breiding, & Likang, 2017). One of the immediate consequences of TBI is an elevated risk of balance deficit or the loss of postural control (Kaufman et al., 2006) (Pickett, 2007). Yet, the pathomechanisms of the postural instability remain poorly

understood. To develop effective rehabilitation strategies and prognosticating tools for motor function recovery, we must delve into the neurophysiological processes involved in postural control.

One aspect that could guide us in this direction is the "functional connectivity (FC)" between the cortical regions involved in postural control during the postural control task. FC refers to the statistical interdependencies between the physiological time series of two regions. In the event of a brain injury, the cortical lesion or the axonal damage can disrupt not only the structural integrity of the white matter (WM) system but also the FC between regions (Gratton, Nomura, Pérez, & DEsposito, 2012). Regardless of the type of network (i.e., the physical synaptic connection between the set of neurons or the functional connection between activities of two brain regions), a graph theory-based approach is a promising tool to quantify the FC network organization wherein the whole brain is viewed as a graph with several nodes (e.g., anatomically parcellated region). Using these quantifiable measures to identify the cortical biomarkers of balance deficits in TBI could better guide us in developing intervention strategies. This brings us to three research questions:

1. *How do the functional networks pertaining to the balance perturbation task change due to TBI?*
2. *Are the global task-specific connectivity measures derived using graph-theory highlight specific brain functional impairment related to balance deficits in TBI?*
3. *Are task-based brain FC measures associated with the structural integrity of WM?*

In pursuit of answers to these questions, we look at the graph-theoretical perspective of brain networks. In this framework, the brain connectivity graph is considered as a network made of nodes and edges. Each node corresponds to a cortical region of interest (ROI; based on anatomical/functional parcellation) and the edge corresponds to the strength of the FC between any two connected nodes. Using these fundamental elements of a graph network, graph theory aims at computing several metrics (i.e., node degree, local and global efficiency [GE], clustering coefficient, modularity, etc.) to characterize and study the functional or structural organization of a network of nodes and edges to better understand the neuroanatomical and neurophysiological basis of brain function. A graphical illustration is presented in Figure 1 to describe the basic concepts of network neuroscience related to this study.

In particular, the concept of *functional integration* and *functional segregation* is gaining significant attention in the network neuroscience community (Cohen & DEsposito, 2016; Hagmann et al., 2008; Newman, 2006; Rubinov & Sporns, 2010; Stam, 2014). In this conceptual framework, as shown in Figure 1, the connectivity structure of the brain is considered to be organized in several statistically independent clusters of nodes or subnetworks referred to as *modules*. The nodes in each module are densely connected to each other while being sparsely connected to other nodes of the brain, forming a *community structure* (Sporns, 2013). In this context, the brain must balance its capacity to segregate information within modules to perform a specialized neural function in local circuits, with its ability to integrate information between modules. The functional organization of the brain into modules and their functional integration and segregation are data-driven based on the FC matrix between all nodes (cortical ROIs in this context). Functional segregation tells us how well the nodes within the modules (cortical ROIs in this context) tend to have a statistical dependence between their time-series (Sporns, 2013). Contrarily, functional integration represents the joint processing of specialized information across subnetworks (or *modules*). In the context of our study, we could posit that during the postural perturbation, brain subnetworks or modules must perform segregated functional
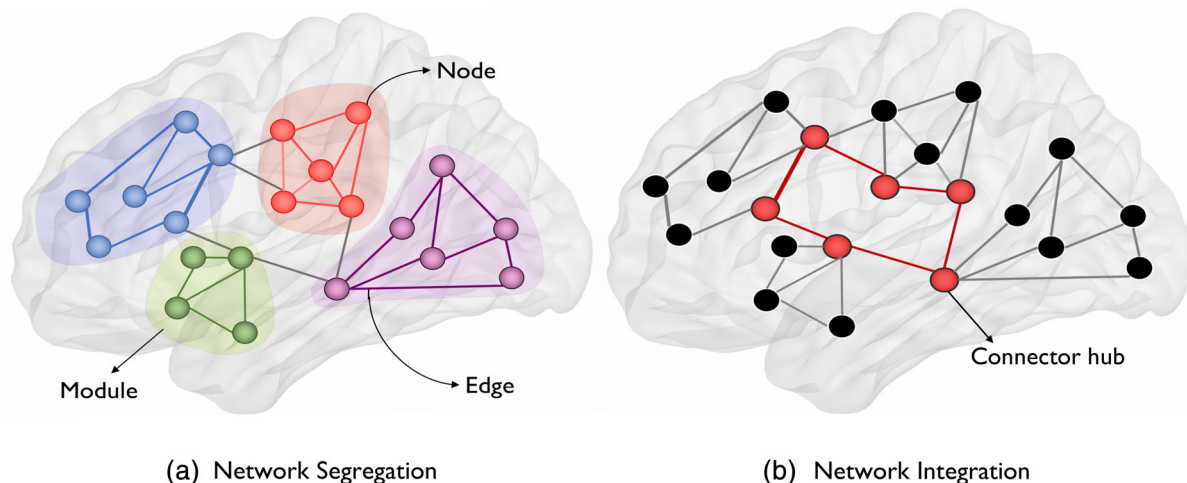

(a) Network Segregation   (b) Network Integration

FIGURE 1 Illustration of graph-theoretic measures. In the context of brain networks in this study, every anatomical region-of-interest is a node, whereas the connection between nodes is termed as an edge. Colored shaded regions correspond to modules which are groups of interconnected nodes but have fewer connections to other modules. On the left, the concept of network segregation is presented as a network comprising of multiple modules (or segregated subnetworks) whereas, on the right, the network integration is illustrated as a group of distant regions interconnected by long-range connections via connector hubs (nodes with a high degree of connectivity)

tasks such as processing visuosensory inputs, planning for the compensatory response, and actually executing the motor response, while maintaining a certain level of sensorimotor integration between modules to execute a timely, well-measured and coordinated response. To better understand the applications of graph theory in neuroscience, we recommend a review by Sporns (2013).

However, to better understand the dynamic aspects of postural control, one needs to study the association between the posturography/balance control measures and the cortical activity recorded during the motor task. The relevant literature on neuroimaging of postural control in a pediatric TBI population is found in Diez et al. (2017) where the postural control indices were reported to be correlated with increased resting-state FC of the prefrontal cortex. In another study by Wang et al. (2016), the postural control change and age were shown to have significant interaction with the prefrontal and sensorimotor connectivity, thus indicating differences in connectivity across age populations. Although these studies demonstrate the correlation between the EEG sensor-based FC and postural control (Edwards, Guven, Furman, Arshad, & Bronstein, 2018; Varghese, Staines, & McIlroy, 2019), sensor-space FC must be interpreted with caution because of its spurious nature associated with the inherent challenge caused by volume conduction; instead, the source-space EEG is recommended for measuring the FC (Bastos & Schoffelen, 2015; Handiru, Vinod, & Guan, 2018; Van de Steen et al., 2016).

For more comprehensive literature on the neuroimaging of human postural control and balance function, readers may refer to the systematic meta-analysis review article (Wittenberg, Thompson, Nam, & Franz, 2017). As most of the aforementioned articles focus only on healthy individuals (young and elderly), the inferences do not offer a complete understanding of balance deficits in the clinical populations suffering from such as TBI and stroke. Moreover, the fMRI-based neuroimaging of the postural task is impractical due to the device constraints of an MRI scanner; thus, EEG offers a unique advantage of being able to noninvasively record the neural recordings while the participant is performing the postural task.

In a preliminary study published by our group, we showed that the N1 amplitude (a type of event-related negative potential) and the center of pressure (COP) displacement were lower in the TBI group as compared to healthy controls (HC; Allexandre et al., 2019). Further, we would like to investigate the changes in cortical connectivity due to postural perturbation in TBI and healthy individuals. We hypothesize that the postural control deficit in TBI could be associated with the altered FC during a balance perturbation task.

While several studies investigated the changes in the cortical activity during the lower-limb motor tasks (Munia, Haider, Schneider, Romanick, & Fazel-Rezai, 2017; Slobounov, Teel, & Newell, 2013; Wittenberg et al., 2017), the current understanding is still inadequate. Not only should we be able to quantify the functional measures using kinematic factors (e.g., trajectory, the COP, limits of stability, etc.) but also be able to complement the underlying neurophysiological mechanism of balance control through different modalities. Thus, in this article, we present a group-level analysis of structural and functional mechanisms of postural instability in TBI patients.

Notwithstanding the published literature on FC changes during postural control tasks in healthy individuals (Varghese et al., 2019;

Wang et al., 2016), the studies are scarce in TBI or other clinical populations. This motivated us to bridge the knowledge gap of the neural correlates of balance deficits in TBI.

The current understanding points to the fact that TBI can cause both focal injuries and diffuse axonal injury (DAI), which disconnects large-scale brain networks (Ham & Sharp, 2012; Sharp, Scott, & Leech, 2014). DAI is commonly induced by a sudden acceleration-deceleration or rotational force, which is mainly affecting WM networks such as corpus callosum and subcortical WM structures (Adams et al., 1989; Basser & Pierpaoli, 1996; Inglese et al., 2005). The injuries are seldom visible on computed tomography (CT) and conventional MRI scans, besides the fact that not many approaches are available to assess the WM damage (Adams et al., 1985). Previous studies have suggested that the DAI is only visible by using advanced neuroimaging techniques that can distinguish microstructural tissue damages (Douglas et al., 2018; Smith et al., 2019). Using diffusion tensor imaging (DTI), WM connectivity, and integrity changes can be identified by several measures of diffusion anisotropy along fiber tracts (Douglas, Iv, et al., 2015; Douglas, Michael, et al., 2015). Fractional anisotropy (FA) measures the directionality of water diffusion or the amount of diffusion asymmetry within a voxel or WM tract. Mean diffusivity (MD) quantifies the total water diffusion, regardless of its direction (Uddin, Figley, Solar, Shatil, & Figley, 2019). Mode of anisotropy (MA) is a measure recently developed to help differentiate the local diffusion profile between a planar disc-like (as in fiber crossing) shape and a linear, cylindrical shape (as in unidirectional converging fibers bundle) (Ennis & Kindlmann, 2005).

DTI approach has been quite promising in evaluating WM DAI. Previous studies have shown that damaged WM due to TBI causes increased MD and reduced FA in WM (Shenton et al., 2012). Our previous work reported the relationship between region-based DTI connectivity (FA values) and physical and cognitive performances in TBI patients (Alivar et al., 2020). Although a few studies have explored the association between motor impairments and WM integrity in TBI populations (Caeyenberghs et al., 2010a, 2010b; Caeyenberghs et al., 2011; Drijkoningen et al., 2015), we would like to further investigate the association between the changes in DTI-based measures and balance deficit-related FC in TBI.

This work aims to study the graph-theoretical properties in an FC graph computed from the source-constructed EEG during a balance perturbation task in TBI. This is the first study to report the changes in functional integration and segregation during a postural control task in TBI to the best of our knowledge. Another key contribution is the investigation of the association between the structural and FC pertaining to postural control in TBI and its relation to balance outcomes.

2 | MATERIALS AND METHODS

2.1 | Participants

In this study, 18 individuals with chronic TBI and 18 HC with no history of brain injury participated. Participants were recruited through our in-house patient information management system and Kessler Institute for Rehabilitation. The definition of TBI was adopted from

the TBI Model Systems National Database ("Identification of Subjects for the TBI Model Systems National Database"), where one of the following criteria must be met (a) loss of consciousness for 30 min or more; (b) posttraumatic anterograde amnesia for 24 hr or more; (c) lowest Glasgow Coma Score (GCS) in the first 24 hr ≤ 15 (unless due to intubation, sedation, or intoxication); or (d) evidence of significant neurological injury on CT/MRI (e.g., subdural hematoma, cerebral contusion, subarachnoid hemorrhage). Severity was further defined using the following GCS score criteria (Teasdale & Jennett, 1974): mild (14–15), moderate (9–13), or severe (3–8). Injury severity was confirmed from medical records when possible; in the absence of medical records, severity was determined by family member attestations of the length of loss of consciousness/coma. Three participants were classified as "moderate/severe" due to the lack of information to make the distinction. Inclusion criteria for participants were they must be: (a) aged between 18 and 65 years, (b) diagnosed with a TBI at least 6 months prior to the participation (as defined above) or be a HC, (c) medically stable in the past 3 months, and (d) be able to stand unsupported for 5 min. Exclusion criteria were as follows: (a) history of lower-limb injury in the past 90 days, (b) history of medication that could affect the balance/muscle coordination, (c) having had any additional orthopedic, neuromuscular, or neurological conditions that could affect balance, (d) having had a penetrating TBI, and (5) have a history of previously diagnosed balance impairments (prior to TBI).

Upon careful visual inspection of the raw EEG data, we excluded the data from four participants (one TBI, three HC) as the signals were too noisy. This resulted in the inclusion of 17 TBI and 15 HC subjects in our EEG data analysis. Our DTI analysis was further limited to a subset sample of 12 TBI and 9 HC because they failed to meet MRI-related inclusion/exclusion criteria or refused to consent to the MRI scan. A summary of the demographics is presented in Table 1.

2.2 | Data acquisition

2.2.1 | MRI data acquisition and processing

A high-resolution T1-weighted (T1-W) image using MPRAGE sequence was acquired using the Siemens Skyra 3 T scanner (Erlangen, Germany) at the Rocco Ortenzio Neuroimaging Center at Kessler Foundation. The following settings were used in the whole-brain volumetric acquisition with the following specifications: 1-mm isotropic voxel resolution, TE = 3 ms; TR = 2,300 ms; 1-mm thick 176 slices; field of view (FOV) 256 × 256 mm^2.

A diffusion weighted (DW) dataset were collected with 64 non-collinear DW gradients with $b = 1,100$ s/mm^2 and 8 $b = 0$ images; matrix size = 128 × 128; FOV = 256 × 256 mm^2; TE = 75 ms; TR = 9,000 ms; isotropic voxel dimensions = 2 mm; and 66 slices. The gradient-echo field map images were acquired to correct for geometrical distortion caused by susceptibility artifacts. The image processing was performed using the FSL 6.0 toolbox that includes: (a) skull stripping using the Brain Extraction Tool; (b) eddy current correction; and (c) DTIFIT diffusion tensors using FDT (FMRIB's Diffusion Toolbox, http://www.fmrib.ox.ac.uk/fsl, Oxford, UK). The generated results include parametric maps of DTI metrics, including MD, MA, and FA. To measure the DTI parameters in WM regions only, we first performed tissue segmentation on T1-W images for each individual. Using FSL FAST (Zhang, Brady, & Smith, 2001), each skull-stripped T1-W image was segmented into three different classes of tissue probability maps namely WM, gray matter, and cerebrospinal fluid, and then transformed into a binary mask of WM using a threshold of 0.7. This threshold was chosen based on a comparison of FA histograms in WM-only and non-WM regions as in Benson et al. (2007). Next, these thresholded WM binary masks were applied to the MNI template-registered FA, MD, and MA maps to extract the global WM FA, WM MD, and WM MA metrics using FSL maths and FSL stats (Smith et al., 2004). Also, the voxel-wise statistical analysis of the FA images was carried out using the tract-based spatial statistics (TBSS) (Smith et al., 2006) tool from FSL. First, all the FA data across subjects were aligned to the high-resolution FMRIB58_FA standard space image using the nonlinear registration (Andersson, Jenkinson, Smith, et al., 2007; Smith et al., 2007), and subsequently mapped into a 1 × 1 × 1 mm standard space. These data were then averaged across subjects to obtain the group's mean FA image, from which the mean FA skeleton was derived as a reflection of the center of fiber bundles. An FA threshold value of 0.2 was used for the FA skeleton to exclude tracts with high variability among subjects as well as gray matter and poor WM representations (Smith et al., 2006). Finally, the subject-specific FA images were projected onto the mean FA skeleton to perform a between-group analysis with the FSL function "randomize"

TABLE 1 Summary of participant characteristics

Parameters	TBI	HC	p-Value
N	17	15	
Severity	Mild = 3; moderate = 3;	NA	NA
	Moderate/severe = 3; severe = 8		
Years post injury (mean, range)	10.04, [1.67, 57.87]	NA	NA
Age (mean ± SD)	48.7 ± 12.5	47 ± 12.8	.7
Gender (M/F)	13/4	8/7	
Height in cm (mean ± SD)	177.3 ± 8.6	171.9 ± 10.8	.13
Weight in kg (mean ± SD)	90.87 ± 22.8	78.26 ± 19.4	.11

Abbreviations: HC, healthy controls; TBI, traumatic brain injury.

and the threshold-free cluster enhancement and family-wise error corrected at $p < .05$ (Salimi-Khorshidi, Smith, & Nichols, 2011). In addition to FA, diffusivity maps based on MD and MA were created as described above.

2.2.2 | Postural data acquisition and processing

A computerized dynamic posturography (CDP) platform (NeuroCom Balance Master, NeuroCom Intl, Clackamas, OR) as shown in Figure 2 was used to study the neural and postural response to unpredictable balance perturbations. Henceforth, we use the term "CDP platform" and "balance platform" interchangeably. The participants were asked to stand on the balance platform, and they were subject to five blocks of random, unpredictable perturbations in the anterior (forward) and posterior (backward) sinusoidal perturbations at 0.5 Hz, (two cycles for a total of 4 s duration) at low (0.5 cm) and high (2 cm) amplitude with an inter-trial separation of 4–8 s. Thus, there are 2×2 combinations of perturbation—anterior and posterior (direction), low and high (amplitude). We measured the COP time series from the ground reaction force data. The COP data were epoched, low-pass filtered (10 Hz), detrended, and averaged across trials and conditions for each subject. The COP displacement was computed as the cumulative distance traveled by the trial average COP in the anterior/posterior direction for the first 2 s of the balance perturbation. In this article, our analysis is limited to the high amplitude perturbation in the posterior direction, which led to greater instability across all subjects.

2.2.3 | EEG data acquisition

Throughout the duration of the task, the brain activity was recorded using the 64-channel EEG system (ActiCAP BrainAmp standard, Brain Products, Munich, Germany) positioned according to the International
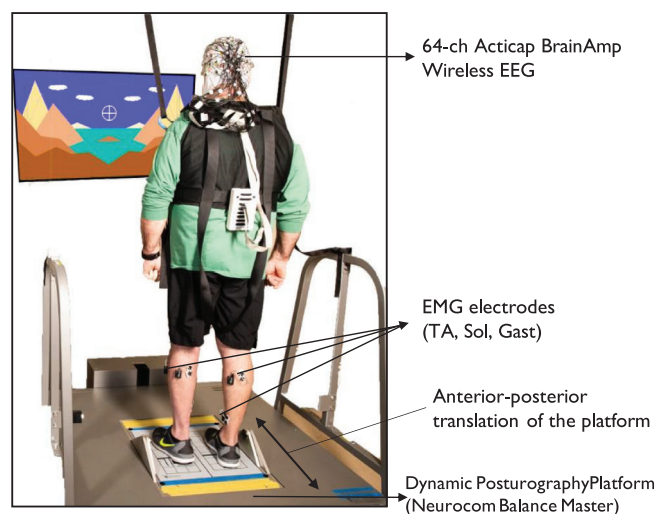

FIGURE 2 A representative subject standing on the dynamic posturography platform used in the study

10–20 systems where the electrode "FCz" and "AFz" serve as the common reference and ground respectively. EEG data were sampled at 500 Hz and the skin-electrode contact impedance was ensured to be below 20 k ohms by applying electrode gel. The EEG electrode positions were 3D digitized using the Brainsight navigation system.

2.3 | Data processing

2.3.1 | EEG data preprocessing

EEG recordings were analyzed offline using the EEGLAB toolbox (Delorme & Makeig, 2004). The raw EEG signals were first down-sampled to 250 Hz, followed by band-pass filtering between 1 and 50 Hz using a fourth-order Butterworth filter. Thereafter, the line noise was removed using the Cleanline plugin for EEGLAB; artifact-contaminated channels and noisy continuous-time segments were removed using the artifact subspace reconstruction (ASR) plugin for EEGLAB (Mullen et al., 2015). The ASR parameter to reconstruct the high variance subspace was set as 20 based on the findings reported in Chang, Hsu, Pion-Tonachini, and Jung (2020). Subsequently, we performed the independent component analysis via extended Infomax algorithm (Makeig, Bell, Jung, & Sejnowski, 1996). The resulting ICs presumably originated from the following physiological or miscellaneous sources—brain, muscle, eye, line noise, channel noise, heart, or other—were labeled accordingly with the ICLabel plugin in the EEGLAB toolbox (Pion-Tonachini, Kreutz-Delgado, & Makeig, 2019). The ICLabel is a machine learning approach, which has been trained to classify the ICs derived from EEG data based on several characteristics such as spectral properties, brain topography. Furthermore, to validate the ICs supposedly generated by neural sources, the DIPFIT tool (available in EEGLAB) was used that localizes the dipoles within the brain volume (Delorme, Palmer, Onton, Oostenveld, & Makeig, 2012; Oostenveld & Oostendorp, 2002). In our study, we only retained the ICs that were (a) identified as "Brain" by the ICLabel plugin and (b) having a residual variance of <15% after localization by DIPFIT modeling. Although we used the ICLabel for automating the labeling of ICs, we also visually inspected whether the characteristic topography and spectral properties of ICs corroborated with their respective labels. Once the ICs were selected, we used the back-projected sensor EEG for source localization. The EEG data processing pipeline is summarized in the block diagram shown in Figure 3.

2.3.2 | EEG source localization and FC estimation

EEG source localization (ESL) allows one to study the cortical dynamics using the underlying cortical sources estimated from the sensor-space EEG (Handiru et al., 2018; Michel & Brunet, 2019). As shown in Figure 3, ESL is implemented in two stages: forward and inverse modeling. Forward modeling is done to compute the volume conduction model, which realistically approximates the electromagnetic field propagation through different layers in the head model (scalp, skull,
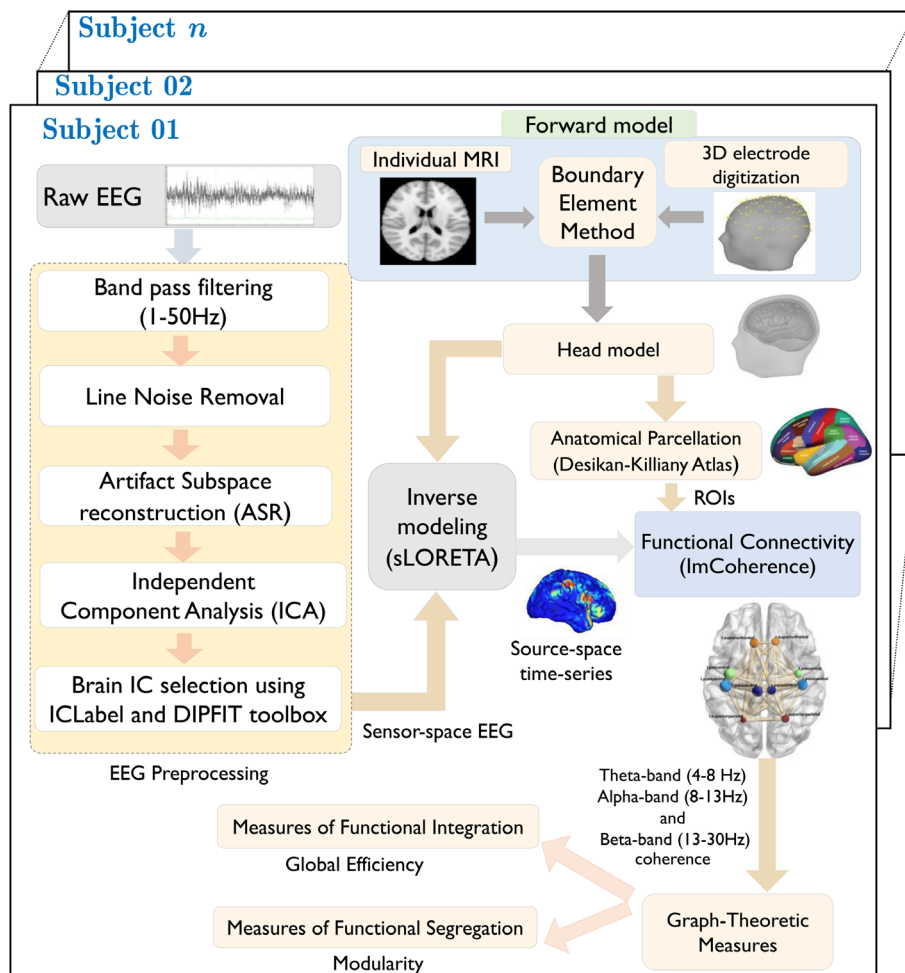
cerebrospinal fluid, gray matter, and WM). Using the subject-specific anatomical data comprising of T1-weighted MRI ad 3D digitized EEG positions, a realistic forward model is created using the Boundary Element Method (Fuchs, Drenckhahn, Wischmann, & Wagner, 1998; Gramfort, Papadopoulo, Olivi, & Clerc, 2010). Inverse modeling based on standardized low-resolution electromagnetic tomography algorithm (Pascual-Marqui, 2002) is used to compute the cortical time series data. More mathematical details of the ESL can be found in the supplementary material (Section S1). All the aforementioned steps were implemented using Brainstorm software (Tadel, Baillet, Mosher, Pantazis, & Leahy, 2011).

Once the source time series is obtained, we computed the ROI time series by averaging the time-series of all the voxels with each anatomical region parcellated according to the Desikan–Killiany Atlas. Between each ROI, we then estimated the FC using imaginary coherence $\text{Im}(\underline{\Gamma})$ with $\underline{\Gamma} \in \mathbb{C}^{U \times U \times V}$ being a three-way tensor, where U and V are the number of ROIs and frequency bins of interest, respectively. In this study, $\text{Im}(\underline{\Gamma})$ is computed during the *baseline* ($t = -2$ to 0 s) and *task* ($t = 0$–2 s) period for each frequency bin and averaged across frequencies to obtain coherence measures for the theta band (4–8 Hz), alpha-band (8–13 Hz), and beta-band (13–30 Hz), given their distinct role in sensorimotor function (Buchholz, Jensen, & Pieter

Medendorp, 2014; Omlor, Patino, Mendez-Balbuena, Schulte-Monting, & Kristeva, 2011).

2.3.3 | Graph-theoretic measures

As mentioned earlier, the *functional segregation* informs about the local network properties, such as how densely connected are the subnetworks (or *modules*) (Newman, 2006) (Figure 1a). On the other hand, *functional integration* captures the information about the ease of interaction between these subnetworks (Figure 1b). The following graph-theoretic measures to characterize the functional segregation and integration of the network were computed for theta-, alpha-, and -beta-band connectivity. The weighted rather than the binary definition of the connection or edge between nodes are used, which is defined as the normalized connectivity strength with values between 0 and 1 (Rubinov & Sporns, 2010).

The measure of functional integration
Global efficiency: It describes how well connected is the neighborhood of a node. It is a measure of the efficiency of information transfer among all pairs of nodes in a graph, given by:

$$GE = \frac{1}{N(N-1)} \sum_{i,j \in G} \frac{1}{d_{ij}^w} \quad (1)$$

where N denotes the number of nodes in a graph G and $d_{ij}^w = \sum_{a_{uv} \in g_{i \to j}^w} f(w_{uv})$ denotes the shortest weighted path length between the nodes i and j in a graph G computed using the Djikstra's algorithm. $g_{i \to j}^w$ corresponds to the shortest weighted path between the nodes i and j, and $f(w_{uv})$ denotes the mapping from connection weight to the path length (i.e., $f(w_{uv}) = (w_{uv})^{-1}$). In the context of brain connectivity, w_{uv} is the imaginary coherence value measured between the nodes u and v. Greater GE would reflect overall more direct communication that is, shorter path length between nodes.

The measure of functional segregation

Modularity (M) is a measure of functional segregation that describes the *community structure* of a network (Newman, 2006). It compares the number of connections within *modules (or subnetworks)* to the number of connections across *modules*. Although there are different ways to compute the modularity, here we used Newman's algorithm as provided in the BCT toolbox (Rubinov & Sporns, 2010). The modularity score Q^w for a weighted connection matrix can be computed as follows:

$$Q^w = \frac{1}{l^w} \sum_{i,j \in N} \left[w_{ij} - \frac{k_i^w k_j^w}{l^w} \right] \delta_{m_i m_j} \quad (2)$$

where l^w is the sum of all weights in the given network (i.e., $l^w = \sum_{i,j} w_{ij}$), also defined as the network strength (NS). k_i^w and k_j^w denote the weighted node degree of nodes i and j, respectively (i.e., $k_i^w = \sum_{j \in N} w_{ij}$). m_i and m_j define the module containing the nodes i and j, respectively. $\delta(m_i, m_j)$ defines the community structure, that is, $\delta_{m_i m_j} = 1$, if both nodes i and j belong to the same community.

2.4 | Statistical analysis

The normality assumption for all the data distribution was verified using visual inspection and the Shapiro–Wilk test with a significance level of $\alpha = .05$. Based on the data distribution, the analysis was performed using parametric or nonparametric statistics.

We performed the two-sample t test to compare the demographics characteristics (age, height, and weight) and the COP displacement. As the normality assumption was not met for the Berg Balance Scale (BBS), we performed a nonparametric statistical test (Wilcoxon rank-sum test) for cross-group BBS comparisons.

To investigate the cortical regions involved during the balance perturbation task, we performed a nonparametric permutation test (Maris & Oostenveld, 2007) at the population level (TBI and HC) to identify significant voxel differences between the task period ($t = 0$–2 s) and baseline period ($t = -2$ to 0 s) in each frequency band. As a frequentist approach, the nonparametric permutation test does not assume a specific distribution of the data. In the randomization procedure, the group-averaged values of the cortical activity during the task at each voxel within each group (TBI and HC) were permuted 1,000 times to generate a randomized distribution. For each permutation, the empirical value based on the paired Wilcoxon signed-rank statistics of the nonpermuted data was compared with the statistics obtained from permuted distribution. The number of times the permuted statistic exceeding the empirical value divided by the total number of permutations ($N = 1,000$) was used as the p-value. To correct for the multiple comparisons, we used the false discovery rate correction based on the Benjamini–Yekutieli procedure (Benjamini & Yekutieli, 2001) which is shown to be robust even under an arbitrary dependency structure in the data.

Regarding the FC features, each imaginary coherence value (FC measure) between any two nodes (or ROIs) for each subject was tested for its statistical significance using Schelter's approach (Schelter et al., 2006) as implemented in the Brainstorm toolbox. Only significant connections were retained for further analysis of connectivity strength and graph measures.

Since the data distribution turned out to be either normal or pseudo-normal for the graph metrics, we performed a two-way repeated-measures analysis of variance (2×2 rmANOVA) using a general linear model, to compare across groups (TBI vs. HC) and time (*baseline* period between -2 and 0 s and balance perturbation *task* period between 0 and 2 s) for each frequency band. Whenever an overall significant effect was found, corresponding post hoc analyses using a two-tailed t test were performed to examine between-group differences at baseline and/or during the task, between-group changes over time, and/or changes within the group. The effect sizes are reported using Cohen's d (for t test) and partial eta-squared (η_p^2 for rmANOVA) values. The statistical analyses related to ANOVA and t test were performed with SPSS (version 26, IBM, NY), with the significance level set at $\alpha < .05$.

Furthermore, to determine whether network measures are associated with the behavioral measures, we calculated the Pearson correlation. In the case of correlation analysis, we identified the influential data points using a commonly accepted criterion of cook's distance $>4/N$ (Cook, 1977), where N is the number of data points in the regression model. The corrections for multiple correlations were done using the Bonferroni correction.

3 | RESULTS

3.1 | Participants characteristics and balance outcomes

A two-tailed t test revealed no significant differences in the baseline demographics (age, height, and weight) characteristics, as shown in Table 1. With regard to the functional outcome measures, as shown in Figure 4, TBI group showed a significantly ($t = 3.07$, $p = .004$, Cohen's $d = 1.09$) larger COP displacement (mean $\pm$ SD $= 11.64$ ± 4.28, 95% CI $=$ [4.79, 19.18]) as compared to HC (mean $\pm$ SD $= 7.82 \pm 2.33$, 95% CI $=$ [4.7, 13.13]). Due to the non-normal distribution of the BBS, we ran a Wilcoxon rank-sum test to compare the BBS of both groups. We observed a significantly lower BBS
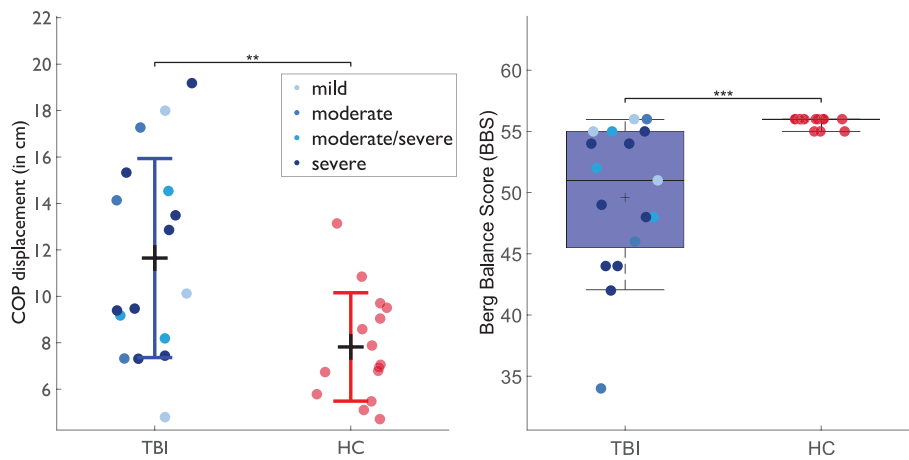
($p = .007$, $z = 2.68$) in TBI (median, range = 51, [34, 56]) than HC (median = 56, range = [55, 56]).

3.2 | Task-induced cortical activity during balance perturbation

The spatial distributions of the significant voxels in different frequency bands are shown in Figure 5. The *w*-values (in the color bar) denote the Wilcoxon signed-rank statistic (sum of the positive or negative ranks).

3.3 | Two-way rmANOVA

3.3.1 | Whole-brain FC network strength

Figure 6 shows the *non-normalized* FC and *non-normalized* node strength for each ROIs (defined as the sum of connectivity values to all other ROIs, i.e., how strongly connected that ROI is) based on source-space EEG coherence in the theta- and alpha-bands during the baseline period as well as during the balance perturbation task in TBI and HC.

The two-way rmANOVA conducted on the graph measures are summarized in Table 2 and the descriptive statistics in Table 3. Theta coherence-based NS showed a main effect of *Time*, but only a marginal nonsignificant *Group* effect and no *Group* × *Time* interaction. Within-group two-tailed *t* test revealed a significant baseline to task change for both the groups (TBI and HC). Between-group contrast analysis revealed a greater NS in HC compared to TBI at baseline (Figure 6).

When comparing the alpha-band NS, two-way rmANOVA revealed a significant main effect of *Time* as well as *Group*, but no significant *Group* × *Time* interaction. Between-group contrast analysis revealed a lower NS (alpha-band) in TBI compared to HC during the task as well as the baseline (Figure 6).

We did not find any significant differences with the beta-band results, but they are included in supplementary materials (Table S1)
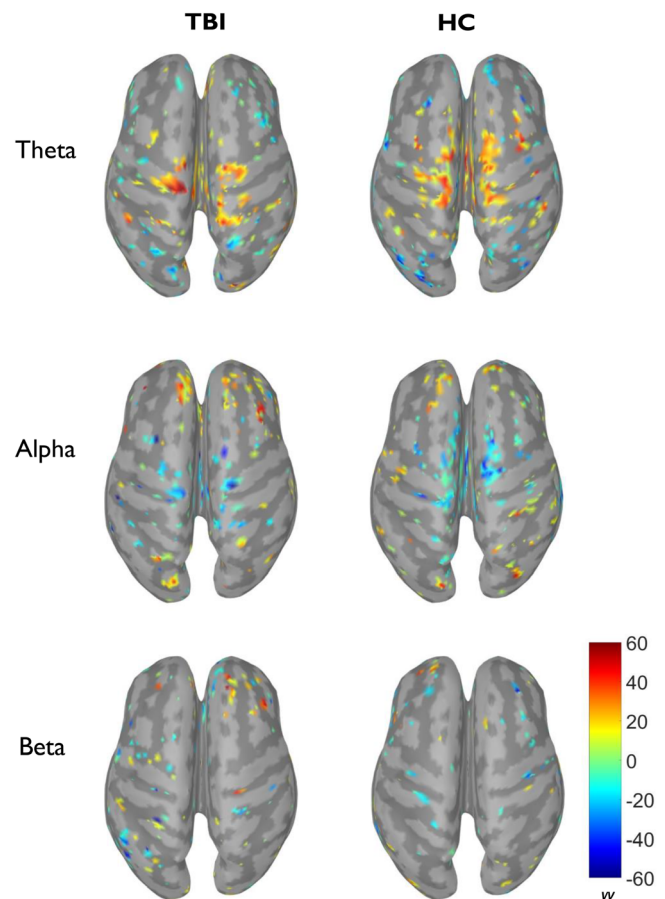

FIGURE 5 Spatial distribution of task-specific significant voxels mapped onto the cortex within each group. Nonparametric permutation-based tests ($N = 1,000$ iterations) are used to identify the voxels that are significantly different from the task period ($t = 0$–2 s) as compared to the baseline period ($t = -2$ to 0 s). False discovery rate (FDR) correction is done using the Benjamini–Yekutieli procedure with the significance level of $\alpha = .05$

for the sake of completion. Overall, we observed a pattern of globally weaker connectivity and weaker node strength in TBI compared to control.
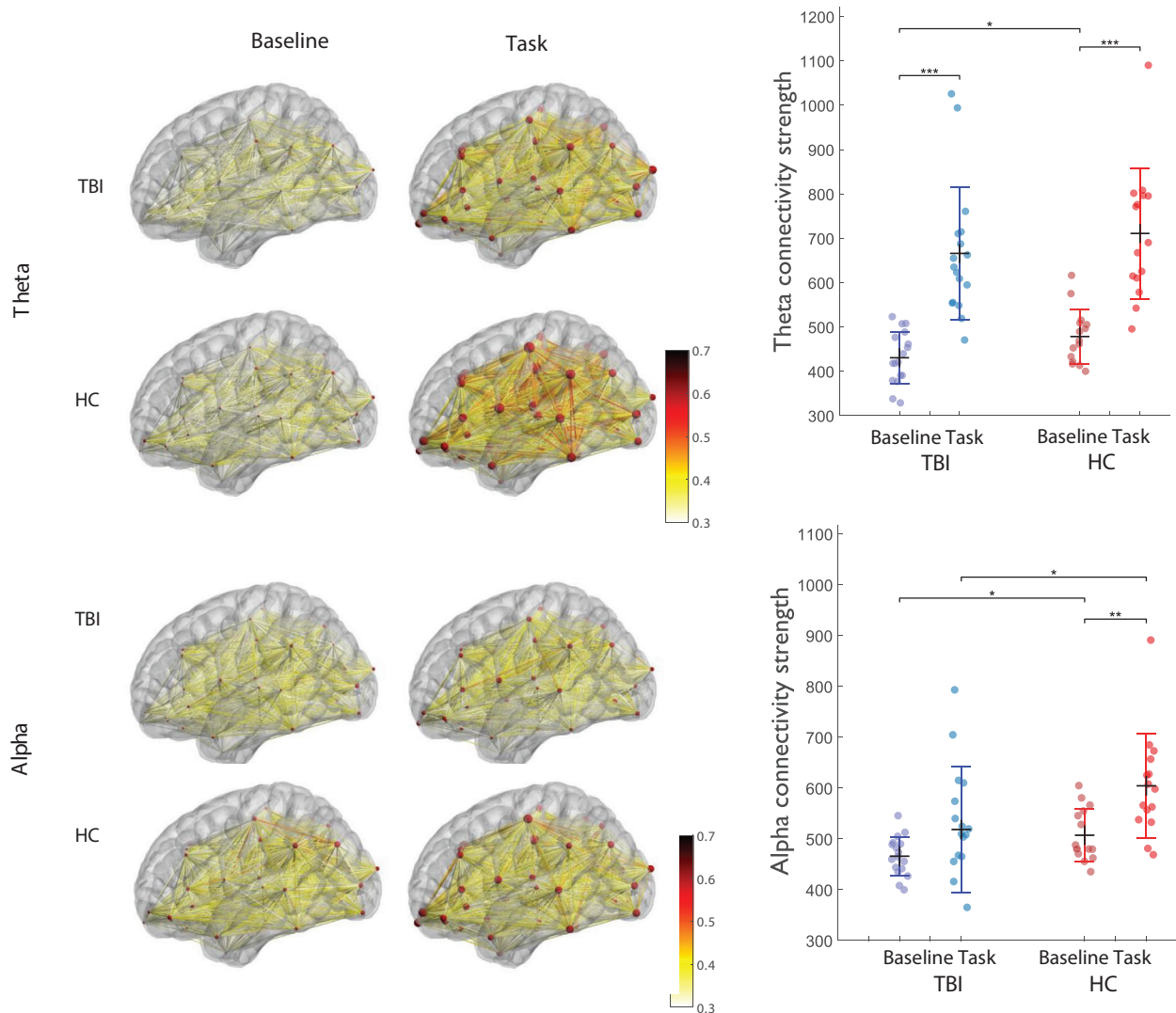
FIGURE 6 Whole-brain functional connectivity based on source-space EEG coherence in different frequency bands in each group (traumatic brain injury [TBI] and healthy controls [HC]) across time periods (baseline and task). Group-level connections are averaged and plotted as an edge between different ROIs anatomically parcellated using Desikan–Killiany Atlas. For better visualization, the connections are thresholded at edge weight = 0.3. Seed voxels of each ROI are indicated as spheres with a radius proportional to their node strength. On the right side, the boxplot comparison of network strengths during the baseline versus task period is shown for both the groups. Statistically significant differences are highlighted with asterisk * ($p < .05$), ** ($p < .01$), *** ($p < .005$), and marginally significant difference is highlighted with a † ($p < .1$). Visualization of the cortical map is done with the help of BrainNet Viewer (Xia, Wang, & He, 2013)

3.3.2 | Graph measures of functional integration and segregation

Global network measures of functional integration and segregation were measured using the GE and modularity (M), respectively, in different frequency bands (during the *baseline* and balance perturbation *task*) for each group. The boxplot summary of the group-level comparison is shown in Figure 7. The results for beta-band coherence connectivity were not significant, but for the sake of completeness, they are included in the supplementary material (Tables S1 and S2).

Functional integration

The two-way rmANOVA was conducted on GE independently for each of the frequency bands. Theta coherence-based GE showed a significant main effect of *Time* and a marginal effect of *Group*, but no significant *Group* × *Time* interaction. As illustrated in Figure 7, the within-group post hoc analysis revealed a significant *baseline* to *task* change in GE for both the groups.

In the case of alpha-band GE, the two-way rmANOVA showed a significant main effect of Group but with no significant *Time* effect or *Group* × *Time* interaction. Moreover, the within-group post hoc analysis revealed no significant *baseline* to *task* change in GE for either group.

TABLE 2 Summary of two-way repeated measures ANOVA

		$F_{(1,30)}$	p	Effect size	$F_{(1,30)}$	p	Effect size	$F_{(1,30)}$	p	Effect size
Network strength	Theta	3.13	.09	0.095	58.9	**.0001**	0.66	0.002	.96	0.0001
	Alpha	9.07	**.005**	0.23	11.07	**.002**	0.27	0.98	.33	0.032
Global efficiency	Theta	3.05	.09	0.092	52.8	**.0001**	0.64	0.035	.96	0.0004
	Alpha	8.86	**.006**	0.23	1.02	.32	0.032	0.17	.68	0.006
Modularity	Theta	3.78	.06	0.11	28.6	**.0001**	0.49	0.42	.52	0.014
	Alpha	1.31	.26	0.042	14.6	**.001**	0.33	3.52	.07	0.105

Note: Effect size is denoted using partial eta squared values (η_p^2). Significant p-values ($p < 0.05$) are highlighted in bold.
Abbreviation: ANOVA, analysis of variance.

TABLE 3 Descriptive statistics and contrast analysis of graph measures

			Baseline	Task	Within-group
Network strength	Theta	TBI	431 ± 59	666 ± 150	**t = 6.02, p = 10e-5, d = 1.32**
		HC	478 ± 61	711 ± 147	**t = 5.64, p = 10e-5, d = 1.41**
		Between group	**t = 2.2, p = .04, d = 0.98**	t = 1.02, p = .32, d = 0.45	
	Alpha	TBI	466 ± 38	519 ± 125	t = 1.66, p = .11, d = 0.4
		HC	507 ± 51	605 ± 102	**t = 3.3, p = .003, d = 0.8**
		Between group	**t = 2.6, p = .01, d = 0.91**	**t = 2.11, p = .04, d = 0.75**	
Global efficiency	Theta	TBI	0.36 ± 0.04	0.45 ± 0.05	**t = 1.34, p = 10e-5, d = 5.4**
		HC	0.38 ± 0.29	0.47 ± 0.05	**t = 5.62, p = 10e-5, d = 1.23**
		Between group	t = 0.94, p = .35, d = 0.41	t = 1.9, p = .07, d = 0.83	
	Alpha	TBI	0.39 ± 0.02	0.39 ± 0.043	t = 0.49, p = .63, d = 0.1
		HC	0.41 ± 0.024	0.042 ± 0.045	t = 1.07, p = .29, d = 0.25
		Between group	**t = 2.14, p = .04, d = 0.76**	t = 1.74, p = .09, d = 0.62	
Modularity	Theta	TBI	0.05 ± 0.01	0.034 ± 0.02	**t = 3.27, p = .002, d = 0.82**
		HC	0.048 ± 0.01	0.025 ± 0.01	**t = 5.07, p = 10e-5, d = 1.07**
		Between group	t = 0.99, p = .33, d = 0.35	t = 1.54, p = .13, d = 0.54	
	Alpha	TBI	0.044 ± 0.01	0.039 ± 0.01	t = 1.1, p = .28, d = 0.3
		HC	0.044 ± 0.01	0.029 ± 0.01	**t = 3.3, p = .003, d = 1.2**
		Between group	t = 0.12, p = .90, d = 0.04	t = 1.9, p = .06, d = 0.67	

Note: Between group ($df = 30$); within-group TBI ($df = 32$), within-group HC ($df = 28$), d: effect size is denoted using Cohen's d value. Bold values represent significant p-values ($p < .05$).
Abbreviations: HC, healthy controls; TBI, traumatic brain injury.

Functional segregation

To investigate the task and group effect on functional segregation, the two-way rmANOVA comparison was performed on the modularity (M) values derived from different frequency bands. We noticed a significant effect of *Time* and *Group* for Theta-band *M*, but no *Group* × *Time* interaction. The post hoc within-group analysis showed a significant *baseline* to *task* decrease within both groups.

In the case of alpha coherence-based *M*, there was a significant effect of *Time* and a marginally significant *Group* × *Time* interaction but not of *Group*. Indeed, as shown in Figure 7, regions are functionally less segregated during the balance perturbation *task* compared to *baseline* for HC but not for TBI. The post hoc analysis of baseline to task change in alpha modularity revealed a marginally significant difference ($p = .067$) between HC ($-0.015 ± 0.013$) and TBI (-0.005

± 0.017). Intuitively this suggests that during the perturbation task, more cortical areas (aka "network node") are interacting with each other in HC, thus reducing the functional segregation, but not in TBI. Given the lack of significance of beta-band results, we have included the results in the supplementary material.

3.4 | Group differences in global DTI measures

Changes in structural networks were assessed by performing group comparison of the global measures of DTI as FA, MD, and MA computed for the whole brain for the subset of 12 TBI and 9 HC with DTI data. All three metrics showed significant differences in the structural integrity between TBI and HC subjects (see Figure 8a). More
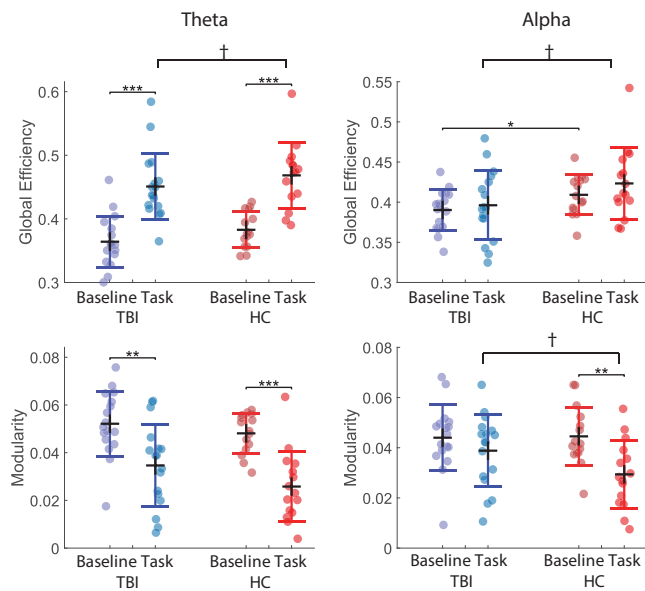
FIGURE 7 Group-level comparison of network measures of functional integration (top half) and functional segregation (bottom half) across frequency bands. The categorical scatter plot of the network measures during the baseline and during perturbation (task) within each group is shown above. Black horizontal line indicates the mean and the colored horizontal lines indicate the *SD*. Statistically significant differences are highlighted with asterisk * (*p* < .05), ** (*p* < .01), *** (*p* < .005), and marginally significant difference is highlighted with a † (*p* < 0.1)

specifically, the global WM FA is significantly lower ($t(1,19) = 3.4$, $p = .003$, Cohen's $d = 1.49$) in TBI (mean ± *SD* = 0.31 ± 0.026, 95% CI: [0.29, 0.32]) than in HC (mean ± *SD* = 0.35 ± 0.03, 95% CI [0.32, 0.37]). MD values are significantly higher ($t(1,19) = 2.65$, $p = .016$, Cohen's $d = 1.14$) in TBI (mean ± *SD* = 9.25e-4 ± 5e-4, 95% CI: [8.9e-4, 9.6e-4]) than HC group (mean ± *SD* = 8.52e-4 ± 1e-4, 95% CI: [7.9e-4, 9.1e-4]). Also, as shown in Figure 8a, significant difference ($t(1,19) = 2.13$, $p = .046$, Cohen's $d = 0.97$) was observed for the global MA between TBI (mean ± *SD* = 0.29 ± 0.03, 95% CI: [0.27, 0.31]) and HC (mean ± *SD* = 0.32 ± 0.02, 95% CI: [0.3, 0.33]).

To address the structural changes in brain WM between groups, we conducted the voxel-wise analysis for the FA, MD, and MA images using TBSS as shown in Figure 8b. For FA, areas highlighted in red/yellow colors are regions where FA was significantly lower and MD significantly higher (*p* < .05) in TBI compared to HC. Regions affected are widespread and strongly overlap between FA and MD and notably include the corpus callosum, corticospinal tract, and thalamus. No significant difference in MA skeletons was observed between groups.

3.5 | Association between DTI measures and behavioral measures

To explore the underlying association between WM damage and balance, the correlation between DTI global metrics (FA, MD, and MA) and behavioral measures, that is, COP and BBS, in TBI patients were studied.

Given the multiple correlation analyses (three DTI measures × two behavioral measures), we ran the Bonferroni correction with the corrected $p = .05/6$ (i.e., .008). Upon correcting for multiple comparisons, we did not find any correlation that survived the Bonferroni correction.

3.6 | Association between EEG graph-theoretic measures and behavioral measures

To explore the brain-behavioral relation, Pearson correlation coefficients between EEG graph measures in each of the frequency bands and behavioral measures (i.e., COP displacement [in cm] and BBS) within the TBI group were calculated. To avoid spurious results given the small sample size, any outlier with a strong influence on the correlation based on the cook's distance $D > 4/N$ criterion (Cook, 1977) was removed. Both results with and without the outliers are reported for completeness (Figure 9a). As the correlation analyses involved three graph measures (NS, GE, and M) across three frequency bands, and two behavioral measures (COP and BBS), we did the Bonferroni correction for multiple comparisons with the corrected *p*-value being $p = .05/18$ (i.e., .0027). Upon correcting for multiple comparisons, we only observed a significant negative correlation between the theta modularity and BBS ($r = -.72$, $p = .001$).

3.7 | Association between global DTI measures and global EEG connectivity graph measures

To explore the underlying association between structural and FC graph metrics during postural control task, the correlation between each of the three functional graph metrics (GE, M, and NS) and global DTI metrics (FA, MD, and MA) were analyzed using the Pearson correlation test. Due to the multiple comparisons (three DTI measures, three graph measures in each of the three frequency bands), the Bonferroni-corrected *p*-value is .05/27 (.002). The correlation between the beta-band NS and the global MA (when outliers were removed: $r = .89$, $p = .0001$) survived the Bonferroni correction. The significance level of the correlation between the beta-band NS and the WM FA was close to the Bonferroni-corrected significance level ($r = .84$, $p = .0023$ without and $r = .73$, $p = .0065$ with outliers). A similar trend (but in the opposite direction) was seen with the correlation between the beta-band NS and the global WM mean diffusivity ($r = -.77$, $p = .0055$ without outliers; $r = -.75$, $p = .0046$ without outliers). Overall, these results suggest a relationship between the structural integrity of the WM system and the strength of the functional connections. For the sake of completion, we report other significant correlations that did not survive the Bonferroni correction in the supplementary material.

4 | DISCUSSION

In this study, we demonstrated the neural correlates of balance deficits using global and topological measures of FC and structural
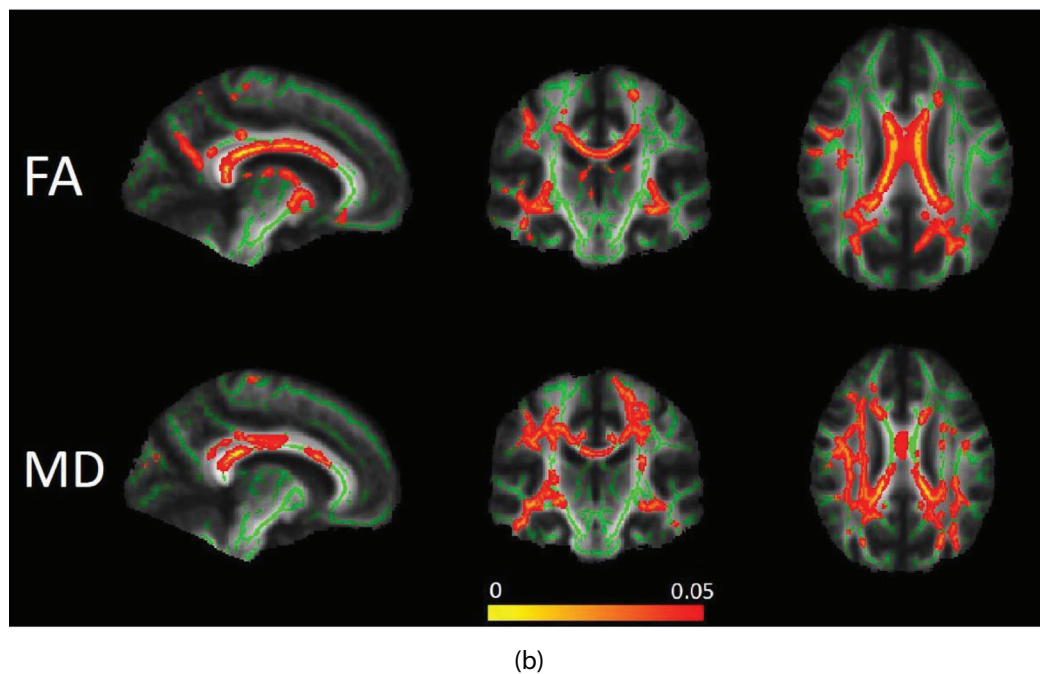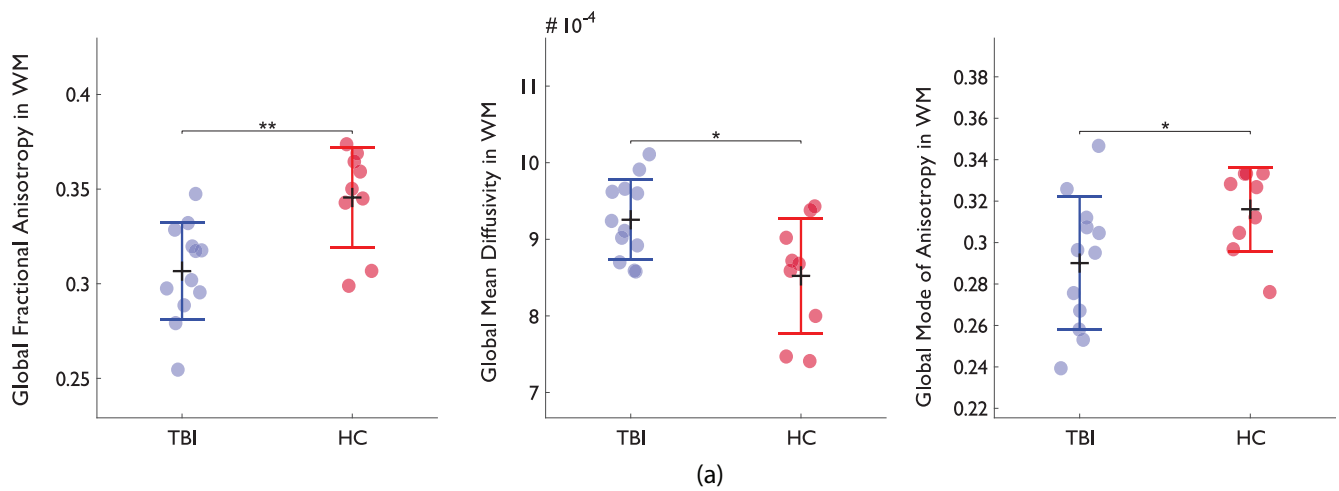
FIGURE 8 (a) Boxplots showing the differences in global diffusion tensor imaging (DTI) measures across groups. Statistically significant differences are highlighted with *($p < .05$), **($p < .01$). (b) Three views (sagittal, coronal, and axial) of significant differences in fractional anisotropy (FA) and mean diffusivity (MD) using tract-based spatial statistics (TBSS) between traumatic brain injury (TBI) and healthy controls (HC) group. The underlying image is the mean FA map, the green contour indicates the mean FA skeleton with a threshold of 0.2, and the red-yellow contours (red showing higher p-values and yellow showing lower p-values) show the regions with significantly ($p < .05$) higher FA values and lower MD values in HC group compared to TBI

integrity of the WM in the TBI population as compared to HC. To the best of our knowledge, this is the first report of EEG-based FC measures during a postural perturbation task in TBI and its association with the altered WM integrity.

4.1 | Effect of TBI on balance

The widely used clinical measure of balance function using the BBS showed an overall balance deficit and a significantly lower BBS score in the TBI population compared to HC. However, there was a wide range of deficits with half of our sample scoring near the healthy maximal values of 56, while the other half below 50, with the knowledge that a score of 45 has been traditionally considered the cut-off for a greater risk of falls (Berg et al., 1992, b).

Similarly, TBI as a group showed significantly greater postural instability, that is, larger COP displacement (i.e., body sway) in response to the balance perturbation compared to HC. This balance impairment is, however, quite variable with half of our TBI population having COP values in the range of those of HC.

Despite a moderate relationship between COP and BBS ($r = -.52$, $p = .03$) in our sample, the two measures may reflect
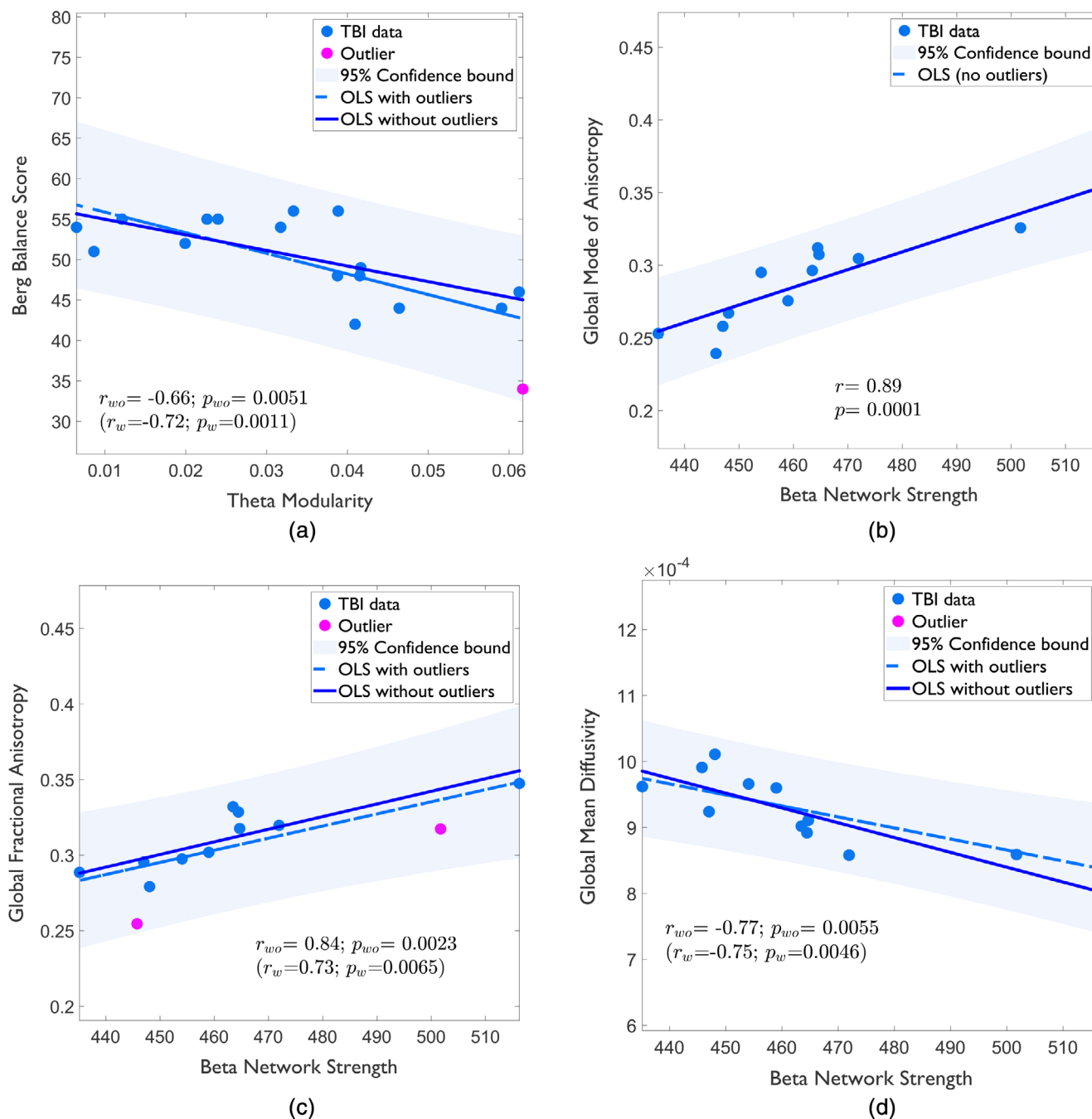
FIGURE 9 Plots of the ordinary least squares regression correlation between the functional outcome measure (Berg Balance Scale [BBS] in the y-axis) and (a) theta modularity in the x-axis. (b) The significant correlations between the beta-band network strength during the postural task within the traumatic brain injury (TBI) group and the global mode of anisotropy in white matter; similarly, (c) the beta-band network strength and global WM fractional anisotropy; and (d) beta-band network strength and global WM mean diffusivity. The effect of outliers on the correlation is highlighted with two separate regression lines (dashed line when outliers are removed, solid line when the outliers are retained). r and p-values indicate the Pearson correlation coefficients and the significance level, respectively. r_w and p_w denote the correlation statistics when outliers are also taken into account; r_{wo} and p_{wo} denote the correlation statistics without outliers

different aspects of balance control. Berg et al. found that BBS was more strongly correlated with functional measures of balance such as timed up-and-go than laboratory measures of body sway during quiet standing or in response to perturbation (Berg et al., 1992, b), which is consistent with our findings from our

group in the same population (Pilkar et al., 2020). The authors suggested that BBS includes various tasks that may capture several and different functional measures of balance impairment, compared to the more controlled environment of laboratory measures (Berg et al., 1992, b). In comparison, the COP displacement

during the balance perturbation measures the ability to dynamically correct external disturbances.

It is finally worth noting that TBI severity at time of injury did not correlate with and therefore, it is not predictive of long-term balance deficit as measured by COP displacement or BBS.

4.2 | Effect of TBI on EEG brain connectivity and graph measures

Postural control is a complex task that relies on the proper functioning of distributed networks of sensorimotor-related brain regions (Takakusaki, 2017). As TBI is often manifested as a DAI, the damage of the WM system can disrupt the whole-brain network connectivity and functioning (Caeyenberghs et al., 2012). Graph theory can help identify alterations in the global brain connectivity organization (Griffa, Baumann, Thiran, & Hagmann, 2013). Previous studies have shown that TBI disrupts the optimal "small-world" architecture of the network (as often observed in the healthy population), affecting the optimal balance between local segregation within and global integration between specialized independent subnetworks (Griffa et al., 2013; Imms et al., 2019; Zhou, 2017). We seek to evaluate how TBI impairs this optimal integration/segregation balance at baseline and during balance perturbation.

4.3 | FC during standing

Our graph-theoretical analysis revealed significantly reduced overall connectivity strength during baseline in the theta-band but not in the alpha or beta-band in the TBI group as compared to HC. This decreased connectivity strength in lower frequency bands is in agreement with (Boshra et al., 2020), who found lower delta and theta connectivity in chronic mild TBI. Another study (Cao & Slobounov, 2010) also observed decreased long-distance connectivity from frontal areas to other parts of the brain, in the alpha band (the only explored band in the study). However, this finding was for acute mild TBI 7 days after the concussion, which may explain the discrepancies with our results. One of the common findings reported in brain disorders is the hyperconnectivity (increased FC) between certain areas within the disrupted network. However, our results contradict the hyperconnectivity hypothesis in TBI (Caeyenberghs, Verhelst, Clemente, & Wilson, 2017) where an increase in connectivity strength or degree has been consistently found in resting-state but also task-based fMRI literature such as in Caeyenberghs et al. 2012 and Diez et al. (2017). Hyperconnectivity is thought to result from an increase in local connection as a need to use detour paths around neurological disruption (Hillary & Grafman, 2017) or a compensatory response for the loss of long-range connections secondary to long-distance fiber tract damage (Venkatesan & Hillary, 2019). The inclusion of more severe and chronic TBI in this study may explain the difference, as it has been argued that more significant disruption from severe injuries or long-term disease progression or age-related degeneration may result in hypoconnectivity (decreased connectivity)

due to structural resource loss (Boshra et al., 2020; Hillary & Grafman, 2017). This was illustrated in Boshra et al. (2020) where EEG-based hyperconnectivity was observed in acute mild TBI and hypoconnectivity in a chronic mild TBI. Alternatively, the brain imaging modality (e.g., EEG vs. fMRI) might be a factor confounding this observation as suggested in Stam (2014), especially given that TBI may alter the relationship between neural activity (EEG) and hemodynamics (fMRI) (Medaglia, 2017). Another possible reason for the discrepancy is that the brain networks are still involved in active control of balance during quiet standing. Also, during this *baseline* period, sensorimotor networks are considered to be involved in anticipatory processing of the forthcoming postural perturbation (Varghese et al., 2019).

4.4 | Task effect

Regarding the balance task-related cortical activity, even though the band-specific spatial pattern of activation is overall consistent between groups, its amplitude is modulated differently by the task. We observe a task increase in theta-band power suggesting an event-related synchronization and a task decrease in alpha-band power indicating an event-related desynchronization in both groups but of larger magnitude in HC. This band specific task modulation is consistent with the findings from an EEG-based balance perturbation study in healthy volunteers (Peterson & Ferris, 2018). In terms of the functional mapping, based on the visual inspection, we observed that most of the significant voxels showing the contrast in theta and alpha-bands are located in the midline central regions (e.g., paracentral lobule, superior parietal lobule, and cingulate gyrus) pertaining to the lower-limb motor functions. The role of these regions in postural control is well-documented in the literature. For example, the cingulate gyrus is shown to calibrate the postural response to a challenging continuous task (Goel et al., 2019) and the role of the paracentral lobule in balance control is highlighted in Diez et al. (2017), Goossens, Janssens, Caeyenberghs, Albouy, and Brumagne (2019), Hagmann et al. (2008), and Boisgontier et al. (2017). The involvement of the superior parietal region in detecting postural instability is reported in Slobounov, Wu, and Hallett (2006).

Comparatively, we observed an overall increase in the *network connectivity* strength (NS) from baseline to task with the largest effect observed for theta (Figure 6) consistent with prior findings (Peterson & Ferris, 2019). The increase in NS was similar for both groups for theta, while it was significant only in HC for the alpha band, and nonsignificant for the beta band. This resulted in a close to significant lower alpha and beta NS in TBI compared to HC during the task. These overall results point to impaired modulation of FC in alpha and beta. Prior literature points to the evidence that the alpha oscillations play a role in coordinating the event-related cortical processes in such a way that they inhibit task-irrelevant functional networks but facilitates task-relevant networks (Klimesch, Fellinger, & Freunberger, 2011). Furthermore, the function of alpha rhythms has been implicated in anticipatory sensorimotor events (Babiloni et al., 2014; Talalay, Kurgansky, & Machinskaya, 2018). Similarly, centroparietal beta connectivity and activation have been implicated in attention and

visuosensory processing to assist motor planning and execution (Chung, Ofori, Misra, Hess, & Vaillancourt, 2017). This result is consistent with our findings regarding increased connectivity and areas of activation during the task.

Following our findings discussed above, theta-band activity has shown to increase in the frontocentral and centroparietal regions significantly, mainly when there is an increasing balance task demand (Mierau et al., 2017; Peterson & Ferris, 2018; Solis-Escalante et al., 2019). Frontocentral and frontoparietal theta band connections also play a vital role in postural control by increasing attention and sensorimotor processing to improve error detection and processing for the proper planning and execution of postural movements (Peterson & Ferris, 2019).

Greater activation for TBI, especially in the prefrontal area as seen in the aging population with the increasing postural challenge (Huang, Lin, & Hwang, 2017), would suggest an increased attentional demand and/or more significant cortical effort to maintain balance. We speculate this could be due to more considerable postural instability, possibly as a compensatory response to reduced connectivity. Similarly, the impaired alpha and beta neural activation and network connectivity strength modulation, without a significant impact on the balance control performance in terms of body sway, would suggest that the TBI participants were able to find a compensatory way to maintain balance for our specific balance task.

4.5 | Functional integration

Our findings showed no significant between-group differences at *baseline* in terms of the global network measures of integration, suggesting that the brain dynamics might not vary much due to pathology when there is no task demand. We observed a significant increase in theta band (but not alpha- or beta-bands) GE during the task. This result is consistent with the findings in Huang, Chang, Tsai, and Hwang (2016), where an increase in GE, that is, functional integration, was observed when participants were challenged to stand on a tilted as compared to a level-surfaced stabilometry platform. This functional integration is achieved likely through long *commissural* and *association fibers* linking different brain regions across- and within the hemisphere, respectively (Stam, 2014). In particular, the regions that are activated along the parasagittal line of the brain (e.g., cingulate gyrus, paracentral lobule, parietal cortex) are part of a highly structurally connected backbone and can serve as a "hub" of communication between other regions to facilitate functional integration (Hagmann et al., 2008). The important integrative role of theta is consistent with the view that the neural synchronization at low frequency facilitates distant regions' coordination, especially in response to increased task demands (Babiloni et al., 2017). Interestingly, at baseline, the theta-band GE was lower (marginally significant) in TBI than in HC, but not during the task. We could speculate that the greater increase in theta activity in TBI may reflect the greater effort needed to increase NS and GE during the task, which was lower than HC at baseline.

4.6 | Functional segregation

Concerning the functional segregation, we observed a decrease in modularity during the perturbation task compared to baseline in theta for both groups, in alpha for HC only and none for beta. More specifically, we noticed a significant reduction in the alpha modularity from baseline to task in HC but not TBI. Our conjecture is that greater cognitive demand during the task are likely to result in decreased functional segregation in HC, a finding that is corroborated by Cohen and DEsposito (2016). In HC, the decrease in modularity during balance perturbation could be attributed to the increased complexity that necessitates the merging of network modules segregated during the resting state (Hearne, Cocchi, Zalesky, & Mattingley, 2017). Neuroimaging of stabilometry studies substantiate our findings (Huang et al., 2016; Varghese et al., 2019). Varghese et al. (2019) postulated that the neighboring cortical areas of fronto-centroparietal areas form new short-range connections to meet the increased demand and integration required to maintain balance control. Their findings of decreased modularity during the perturbation-related task compared to baseline were attributed to cognitive processes possibly involved in anticipatory proprioception in healthy individuals. Interestingly, there is a lack of significant change in alpha modularity in TBI compared to HC during the task. This could be the result of axonal damage in TBI, disrupting task-specific connections which might lead to difficulties in integrating different modules.

Regarding the temporal dynamics of brain activity, we construe that these networks are functionally segregated or sparsely connected during the baseline; however, they communicate with each other depending on the demand for tasks. Balance control is a complex task requiring the proper coordination of a wide visuosensory-motor network (Takakusaki, 2017). The visuomotor and sensorimotor networks must quickly integrate the proprioceptive information from the lower limb (perturbation) in the current context of postural response to an external perturbation. As a responsive action, the supplementary motor area and associated systems try to initiate the upright posture control.

4.7 | Association between the EEG graph measures and the functional outcomes (COP and BBS)

Only theta modularity was found to be negatively correlated with BBS, and this correlation was statistically significant after corrections for multiple comparisons between graph and functional measures. This correlation suggests that a decrease in segregation would be associated with increased functional performance (i.e., higher BBS). This is consistent with the proposed important role of theta band as the conduit and SMA as a major hub of information exchange (i.e., decreased segregation) between a wide network of cognitive and visuo-sensorimotor regions to facilitate the proper detection and planning of corrective motor response to balance perturbation (Peterson & Ferris, 2019). Similarly, in a resting-state FC study conducted by Scala et al. (2019), GE was negatively correlated with COP displacement suggesting that the increase in GE would reflect better

postural control. Theta-band modularity at rest was also recently found to be a predictor for motor learning in a sensorimotor learning task (Miraglia, Vecchio, & Rossini, 2018).

Our correlation results remain exploratory, and caution should be exercised in interpreting this observation as causal.

4.8 | Effect of TBI on structural damage

As previously mentioned, TBI can damage the WM structure due to DAI, potentially disrupting global functional network organization and, consequently, motor response. WM structural changes in TBI patients and HC were quantified using global DTI measures. Consistent with previous research studies (Douglas, Iv, et al., 2015; Douglas, Michael, et al., 2015; Hashim et al., 2017; OPhelan, Otoshi, Ernst, & Chang, 2018; Voelbel, Genova, Chiaravalotti, & Hoptman, 2012), we found a significant reduction in global WM microstructural integrity in TBI as reflected by lower FA and MA, and higher MD compared to controls. Reduced WM integrity and tract degeneration have consistently been reported in chronic TBI (Caeyenberghs et al., 2014; Hashim et al., 2017; Wallace, Mathias, & Ward, 2018). Following DAI, WM tract degeneration would lead to greater free water molecules movements, resulting in lower FA and higher MD. Furthermore, reduced MA would signify more disc-like, less cigar-like shape water diffusion, that is, more fiber crossing and less unidirectional fiber bundle (Douaud et al., 2011; Yoncheva et al., 2016), which could reflect the deterioration and thinning of WM tracts.

Furthermore, using TBSS, we compared the WM tracts in skeletonized maps in TBI and HC as a voxel-based group-level analysis for all three measures. Significant group differences were found for FA and MD, but not for MA. WM injury seems to be widespread and strongly overlaps between and FA and MD. In particular, the main regions affected include the thalamus, corticospinal tract, and most of the corpus callosum, which is consistent with prior findings (Hashim et al., 2017; OPhelan et al., 2018; Owens, Spitz, Ponsford, Dymowski, & Willmott, 2018; Veeramuthu et al., 2015). These findings have important implications given the role of the corpus callosum in cross-hemisphere communication and error detection in balance perturbation (Peterson & Ferris, 2018; Peterson & Ferris, 2019) and thalamus and corticospinal tract in balance-related sensory-motor functions (Surgent, Dadalko, Pickett, & Travers, 2019). Future analyses should further investigate the regional and tract-based WM damage and their potential role in balance deficit and abnormal postural response to the perturbation task.

4.9 | Association between DTI and BBS, and DTI and graph measures

There was no statistically significant correlation between the DTI measures computed on the whole-brain WM and the functional outcome measures such as COP and BBS. Our future work will investigate whether diffusivity characteristics in more local tracts would better correlate with posture control impairment in TBI than *global* measures of WM integrity, as previously shown for the middle and inferior cerebellar peduncles (Caeyenberghs et al., 2010a, 2010b).

However, we did notice significant correlations between the DTI measures (FA, MA, and MD) and EEG graph measure (beta-band NS). The findings suggest that the WM integrity was positively associated with the FC strength in beta-band during the balance task. This is supported by Chu et al. (2015), in which the EEG source-based FC (particularly, the high-frequency beta and gamma-band coherence) was shown to be associated with WM connectivity. Interestingly, only the high-frequency bands (beta and gamma) FC was significantly reduced when the structural support was absent, which may explain the observed relation between WM integrity and FC connectivity strength only in beta-band in our study. While we remain cautious in not overinterpreting this result, future studies should further explore the structural–functional correlation in TBI.

4.10 | Limitations and future directions

We acknowledge that our study has some limitations, particularly with the small sample size. Also, there is another limitation concerning the heterogeneity within the sample population; this is particularly challenging in the TBI group because of the varying degrees of injury (mild/moderate/severe) not necessarily correlating with the motor deficits. However, we have tried our best to control for other factors such as age, height, and weight, which contribute to the postural control performance. Similarly, the wide range of balance impairment in TBI with the inclusion of individuals without deficit may have potentially reduced or eliminated a group difference for some outcomes. Future studies may want to have a balance impairment-related inclusion criterion and consider a stronger study design that also compares TBI with and without impairment.

We cannot completely rule out the potential effect of motion artifacts on our results especially for low frequencies (Nordin, David Hairston, & Ferris, 2019). However, source-localized measures and phase coherence rather than channel-based amplitude-based connectivity or activity, are more immune to motion artifacts. Also, the band-specific rather than a broad spatial pattern of activity modulation (Figure 5) as well as the negative rather than positive correlation between COP (movement) and integration, would suggest a true neural response to the task.

While we integrated information available from both task-based neuroimaging using the EEG and the structural imaging using DTI, it is worth highlighting that the FC between the time-series of two regions is often modulated by factors independent from the structural connectivity. An FC measure between two areas can be influenced by the third region with no direct fiber track in between, but still coordinated functionally via cortico-thalamocortical pathways (O'Reilly, Lewis, & Elsabbagh, 2017). We recommend that future studies investigate the causal association between structural and functional connections.

We must acknowledge that we did not compare the graph metrics to the null model in our graph-theoretic analysis. In our defense, we highlight that the choice of the null model plays a critical role, and it can dramatically change the small-world properties of the network (Fallani, Richiardi, Chavez, & Achard, 2014). Moreover, the choice of FC measurement (e.g., correlation/coherence) can also affect the comparison concerning the null model. Nevertheless, unlike the correlation-based FC measurement, which often results in a spurious association between two regions, the coherence-based FC is tested for its statistical significance using Schelter's approach (Schelter et al., 2006). Incorporating these methodological details is our priority in the upcoming graph-theoretic studies.

In this study, our focus has been primarily on the global measures of EEG connectivity graphs. However, the underlying neural mechanisms of the postural control are too complex to summarize with a single statistical value. Depending on the research question, this can be either a strength or a weakness. In our current approach, we attempted to address whether we can identify a type of neural biomarker based on the EEG connectivity graph. While the global graph measures allow us to explore the association between the connectivity-based graph measures and the functional outcomes, it still does not answer questions related to the local characteristics of task-relevant networks. Notwithstanding this limitation, we did explore the local properties based on the weighted node strength and the significant cortical activity in the ROIs to the postural control. Future work will examine the significance of these nodes in terms of local graph properties such as rich-club coefficient and centrality measures and their relation to local structural integrity measures.

5 | CONCLUSIONS

To the best of our knowledge, this is the first study investigating brain network segregation and integration in a TBI population during a postural control task performed on a computerized stabilometric platform. The findings from EEG graph measures in TBI compared to HC revealed altered baseline and task modulation of global graph-theoretic measures of *NS*, *GE*, and *modularity* in the brain functional networks. Interestingly, reduced network connectivity strength and integration, and greater network segregation were correlated with poorer balance performance (COP and BBS) and greater structural brain damage. Findings from the graph measures were found to be frequency bands and region-specific, thus highlighting their distinct role.

The combined use of EEG-based FC measures during the task and the DTI-based structural integrity measures helped provide new insights into the underlying structural–functional mechanisms of postural control in TBI. These observations could pave the way for future research to identify cortical biomarkers of postural control deficits in TBI, thus potentially assisting clinicians and researchers to better understand neuromuscular disorders.

We believe that our findings and inferences from this pilot study should provide directions to future studies on brain connectivity in TBI and other neuropathologies.

DATA AVAILABILITY STATEMENT

All the raw data are not publicly available due to the IRB restrictions. However, the MATLAB scripts and the deidentified preprocessed EEG data supporting this study can be made available upon reasonable requests to the corresponding author.

ORCID

Vikram Shenoy Handiru https://orcid.org/0000-0001-7460-5107
Soha Saleh https://orcid.org/0000-0002-9936-1249

REFERENCES

Adams, J., Hume, D., Doyle, D., Graham, I., Lawrence, A. E., & McLellan, D. R. (1985). Microscopic diffuse axonal injury in cases of head injury. *Medicine Science and the Law, 25*(4), 265–269. https://doi.org/10.1177/002580248502500407

Adams, J., Hume, D., Doyle, I., Ford, T., Gennarelli, A., Graham, D. I., & Mclellan, D. R. (1989). Diffuse axonal injury in head injury: Definition diagnosis and grading. *Histopathology, 15*(1), 49–59. https://doi.org/10.1111/j.1365-2559.1989.tb03040.x

Alivar, A., Glassen, M., Hoxha, A., Allexandre, D., Yue, G., & Saleh, S. (2020). Relationship between DTI brain connectivity and functional performance in individuals with traumatic brain injury. In *2020 42nd Annual International Conference of the IEEE Engineering in Medicine & Biology Society (EMBC)*. IEEE. https://doi.org/10.1109/embc44109.2020.9176130.

Allexandre, D., Hoxha, A., Handiru, V. S, Saleh, S., Easter Selvan, S., & Yue, G. H. (2019). Altered cortical and postural response to balance perturbation in traumatic brain injury—An EEG pilot study. In *2019 41st Annual International Conference of the IEEE Engineering in Medicine and Biology Society (EMBC)*. IEEE. https://doi.org/10.1109/embc.2019.8856645.

Andersson, J. L. R., Jenkinson, M., & Smith, S. (2007). Non-linear registration aka spatial normalisation FMRIB Technical Report TR07JA2. FMRIB Analysis Group of the University of Oxford, 2(1), pp. e21.

Babiloni, C., del Percio, C., Arendt-Nielsen, L., Soricelli, A., Romani, G. L., Rossini, P. M., & Capotosto, P. (2014). Cortical EEG alpha rhythms reflect task-specific somatosensory and motor interactions in humans. *Clinical Neurophysiology, 125*(10), 1936–1945. https://doi.org/10.1016/j.clinph.2014.04.021

Babiloni, C., del Percio, C., Lopez, S., di Gennaro, G., Quarato, P. P., Pavone, L., et al. (2017). Frontal functional connectivity of electrocorticographic delta and theta rhythms during action execution versus action observation in humans. *Frontiers in Behavioral Neuroscience, 11*(February). https://doi.org/10.3389/fnbeh.2017.00020

Basser, P. J., & Pierpaoli, C. (1996). Microstructural and physiological features of tissues elucidated by quantitative-diffusion-tensor MRI. *Journal of Magnetic Resonance Series B, 111*(3), 209–219. https://doi.org/10.1006/jmrb.1996.0086

Bastos, A. M., & Schoffelen, J.-M. (2015). A tutorial review of functional connectivity analysis methods and their interpretational pitfalls. *Frontiers in Systems Neuroscience, 9*(January), 175. https://doi.org/10.3389/fnsys.2015.00175

Benjamini, Y., & Yekutieli, D. (2001). The control of the false discovery rate in multiple testing under dependency. *The Annals of Statistics*, *29*(4), 1165–1188. https://doi.org/10.1214/aos/1013699998

Benson, R. R., Meda, S. A., Vasudevan, S., Kou, Z., Govindarajan, K. A., Hanks, R. A., … Haacke, E. M. (2007). Global white matter analysis of diffusion tensor images is predictive of injury severity in traumatic brain injury. *Journal of Neurotrauma*, *24*, 446–459.

Berg, K. O., Maki, B. E., Williams, J. I., Holliday, P. J., & Wood-Dauphinee, S. L. (1992). Clinical and laboratory measures of postural balance in an elderly population. *Archives of Physical Medicine and Rehabilitation*, *73*, 1073–1080.

Berg, K. O., Wood-Dauphinee, S. L., Williams, J. I., & Maki, B. (1992). Measuring balance in the elderly: Validation of an instrument. *Canadian Journal of Public Health*, *83*(Suppl 2), S7–S11.

Boisgontier, M. P., Cheval, B., Chalavi, S., van Ruitenbeek, P., Leunissen, I., Levin, O., … Swinnen, S. P. (2017). Individual differences in brainstem and basal ganglia structure predict postural control and balance loss in young and older adults. *Neurobiology of Aging*, *50*(February), 47–59. https://doi.org/10.1016/j.neurobiolaging.2016.10.024

Boshra, R., Ruiter, K. I., Dhindsa, K., Sonnadara, R., Reilly, J. P., & Connolly, J. F. (2020). On the time-course of functional connectivity: Theory of a dynamic progression of concussion effects. *Brain Communications*, *2*(2). https://doi.org/10.1093/braincomms/fcaa063

Buchholz, V. N., Jensen, O., & Pieter Medendorp, W. (2014). Different roles of alpha and beta band oscillations in anticipatory sensorimotor gating. *Frontiers in Human Neuroscience*, *8*(June), 446. https://doi.org/10.3389/fnhum.2014.00446

Caeyenberghs, K., Leemans, A., Geurts, M., Taymans, T., Vander Linden, C., Smits-Engelsman, B. C. M., … Swinnen, S. P. (2010a). Brain-behavior relationships in young traumatic brain injury patients: Fractional anisotropy measures are highly correlated with dynamic visuomotor tracking performance. *Neuropsychologia*, *48*(5), 1472–1482. https://doi.org/10.1016/j.neuropsychologia.2010.01.017

Caeyenberghs, K., Leemans, A., Geurts, M., Taymans, T., Linden, C. V., Smits-Engelsman, B. C. M., … Swinnen, S. P. (2010b). Brain-behavior relationships in young traumatic brain injury patients: DTI metrics are highly correlated with postural control. *Human Brain Mapping*, *31*(7), 992–1002. https://doi.org/10.1002/hbm.20911

Caeyenberghs, K., Leemans, A., Geurts, M., Linden, C. V., Smits-Engelsman, B. C. M., Sunaert, S., & Swinnen, S. P. (2011). Correlations between white matter integrity and motor function in traumatic brain injury patients. *Neurorehabilitation and Neural Repair*, *25*(6), 492–502. https://doi.org/10.1177/1545968310394870

Caeyenberghs, K., Leemans, A., Leunissen, I., Gooijers, J., Michiels, K., Sunaert, S., & Swinnen, S. P. (2014). Altered structural networks and executive deficits in traumatic brain injury patients. *Brain Structure and Function*, *219*(1), 193–209. https://doi.org/10.1007/s00429-012-0494-2

Caeyenberghs, K., Leemans, A., Heitger, M. H., Leunissen, I., Dhollander, T., Sunaert, S., … Swinnen, S. P. (2012). Graph analysis of functional brain networks for cognitive control of action in traumatic brain injury. *Brain*, *135*(4), 1293–1307. https://doi.org/10.1093/brain/aws048

Caeyenberghs, K., Verhelst, H., Clemente, A., & Wilson, P. H. (2017). Mapping the functional connectome in traumatic brain injury: What can graph metrics tell us? *NeuroImage*, *160*(October), 113–123. https://doi.org/10.1016/j.neuroimage.2016.12.003

Cao, C., & Slobounov, S. (2010). Alteration of cortical functional connectivity as a result of traumatic brain injury revealed by graph theory ICA and SLORETA analyses of EEG signals. *IEEE Transactions on Neural Systems and Rehabilitation Engineering*, *18*(1), 11–19. https://doi.org/10.1109/tnsre.2009.2027704

Chang, C.-Y., Hsu, S.-H., Pion-Tonachini, L., & Jung, T.-P. (2020). Evaluation of artifact subspace reconstruction for automatic artifact components removal in multi-channel EEG recordings. *IEEE Transactions on Biomedical Engineering*, *67*(4), 1114–1121. https://doi.org/10.1109/TBME.2019.2930186

Chu, C. J., Tanaka, N., Diaz, J., Edlow, B. L., Wu, O., Hämäläinen, M., … Kramer, M. A. (2015). EEG functional connectivity is partially predicted by underlying white matter connectivity. *NeuroImage*, *108*(March), 23–33. https://doi.org/10.1016/j.neuroimage.2014.12.033

Chung, J. W., Ofori, E., Misra, G., Hess, C. W., & Vaillancourt, D. E. (2017). Beta-band activity and connectivity in sensorimotor and parietal cortex are important for accurate motor performance. *NeuroImage*, *144*(January), 164–173. https://doi.org/10.1016/j.neuroimage.2016.10.008

Cohen, J. R., & DEsposito, M. (2016). The segregation and integration of distinct brain networks and their relationship to cognition. *Journal of Neuroscience*, *36*(48), 12083–12094. https://doi.org/10.1523/jneurosci.2965-15.2016

Cook, R. D. (1977). Detection of influential observation in linear regression. *Technometrics*, *19*(1), 15. https://doi.org/10.2307/1268249

Delorme, A., & Makeig, S. (2004). EEGLAB: An open source toolbox for analysis of single-trial EEG dynamics including independent component analysis. *Journal of Neuroscience Methods*, *134*(1), 9–21. https://doi.org/10.1016/j.jneumeth.2003.10.009

Delorme, A., Palmer, J., Onton, J., Oostenveld, R., & Makeig, S. (2012). Independent EEG sources are dipolar. *PLoS One*, *7*(2), e30135. https://doi.org/10.1371/journal.pone.0030135

Diez, I., Drijkoningen, D., Stramaglia, S., Bonifazi, P., Marinazzo, D., Gooijers, J., … Cortes, J. M. (2017). Enhanced prefrontal functional–structural networks to support postural control deficits after traumatic brain injury in a pediatric population. *Network Neuroscience*, *1*(2), 116–142. https://doi.org/10.1162/NETN_a_00007

Douaud, G., Jbabdi, S., Behrens, T. E. J., Menke, R. A., Gass, A., Monsch, A. U., … Smith, S. (2011). DTI measures in crossing-fibre areas: Increased diffusion anisotropy reveals early white matter alteration in MCI and mild Alzheimer's disease. *NeuroImage*, *55*(3), 880–890. https://doi.org/10.1016/j.neuroimage.2010.12.008

Douglas, D. B., Iv, M., Douglas, P. K., Anderson, A., Vos, S. B., Bammer, R., … Wintermark, M. (2015). Diffusion tensor imaging of TBI: Potentials and challenges. *Topics in Magnetic Resonance Imaging*, *24*, 241–251.

Douglas, D. B., Michael, I. V., Douglas, P. K., Anderson, A., Vos, S. B., Bammer, R., … Wintermark, M. (2015). Diffusion tensor imaging of TBI. *Topics in Magnetic Resonance Imaging*, *24*(5), 241–251. https://doi.org/10.1097/rmr.0000000000000062

Douglas, D. B., Ro, T., Toffoli, T., Krawchuk, B., Muldermans, J., Gullo, J., … Wintermark, M. (2018). Neuroimaging of traumatic brain injury. *Medical Science*, *7*(1), 2. https://doi.org/10.3390/medsci7010002

Drijkoningen, D., Caeyenberghs, K., Leunissen, I., Linden, C. V., Leemans, A., Sunaert, S., … Swinnen, S. P. (2015). Training-induced improvements in postural control are accompanied by alterations in cerebellar white matter in brain injured patients. *NeuroImage: Clinical*, *7*, 240–251. https://doi.org/10.1016/j.nicl.2014.12.006

Edwards, A. E., Guven, O., Furman, M. D., Arshad, Q., & Bronstein, A. M. (2018). Electroencephalographic correlates of continuous postural tasks of increasing difficulty. *Neuroscience*, *395*, 35–48. https://doi.org/10.1016/j.neuroscience.2018.10.040

Ennis, D. B., & Kindlmann, G. (2005). Orthogonal tensor invariants and the analysis of diffusion tensor magnetic resonance images. *Magnetic Resonance in Medicine*, *55*(1), 136–146. https://doi.org/10.1002/mrm.20741

Fallani, F. D. V., Richiardi, J., Chavez, M., & Achard, S. (2014). Graph analysis of functional brain networks: Practical issues in translational neuroscience. *Philosophical Transactions of the Royal Society B: Biological Sciences*, *369*(1653), 20130521. https://doi.org/10.1098/rstb.2013.0521

Fuchs, M., Drenckhahn, R., Wischmann, H., & Wagner, M. (1998). An improved boundary element method for realistic volume-conductor modeling. *IEEE Transactions on Biomedical Engineering*, *45*(8), 980–997. https://doi.org/10.1109/10.704867

Goel, R., Nakagome, S., Rao, N., Paloski, W. H., Contreras-Vidal, J. L., & Parikh, P. J. (2019). Fronto-parietal brain areas contribute to the online control of posture during a continuous balance task. *Neuroscience*, *413*, 135–153. https://doi.org/10.1016/j.neuroscience.2019.05.063

Goossens, N., Janssens, L., Caeyenberghs, K., Albouy, G., & Brumagne, S. (2019). Differences in brain processing of proprioception related to postural control in patients with recurrent non-specific low Back pain and healthy controls. *NeuroImage: Clinical*, *23*(May), 101881. https://doi.org/10.1016/j.nicl.2019.101881

Gramfort, A., Papadopoulo, T., Olivi, E., & Clerc, M. (2010). OpenMEEG: Opensource software for quasistatic bioelectromagnetics. *Biomedical Engineering Online*, *9*(1), 45. https://doi.org/10.1186/1475-925x-9-45

Gratton, C., Nomura, E. M., Pérez, F., & DEsposito, M. (2012). Focal brain lesions to critical locations cause widespread disruption of the modular organization of the b. *Journal of Cognitive Neuroscience*, *24*(6), 1275–1285. https://doi.org/10.1162/jocn_a_00222

Griffa, A., Baumann, P. S., Thiran, J. P., & Hagmann, P. (2013). Structural connectomics in brain diseases. *NeuroImage*, *80*, 515–526. https://doi.org/10.1016/j.neuroimage.2013.04.056

Hagmann, P., Cammoun, L., Gigandet, X., Meuli, R., Honey, C. J., van Wedeen, J., & Sporns, O. (2008). Mapping the structural core of human cerebral cortex. *PLoS Biology*, *6*(7), e159. https://doi.org/10.1371/journal.pbio.0060159

Ham, T. E., & Sharp, D. J. (2012). How can investigation of network function inform rehabilitation after traumatic brain injury? *Current Opinion in Neurology*, *25*(6), 662–669. https://doi.org/10.1097/wco.0b013e328359488f

Handiru, V. S., Vinod, A. P., & Guan, C. (2018). EEG source imaging of movement decoding: The state of the art and future directions. *IEEE Systems, Man, and Cybernetics Magazine*, *4*(2), 14–23. https://doi.org/10.1109/msmc.2017.2778458

Hashim, E., Caverzasi, E., Papinutto, N., Lewis, C. E., Jing, R., Charles, O., … Cusimano, M. D. (2017). Investigating microstructural abnormalities and neurocognition in sub-acute and chronic traumatic brain injury patients with normal-appearing white matter: A preliminary diffusion tensor imaging study. *Frontiers in Neurology*, *8*, 97. https://doi.org/10.3389/fneur.2017.00097

Hearne, L. J., Cocchi, L., Zalesky, A., & Mattingley, J. B. (2017). Reconfiguration of brain network architectures between resting-state and complexity-dependent cognitive reasoning. *The Journal of Neuroscience*, *37*(35), 8399–8411. https://doi.org/10.1523/jneurosci.0485-17.2017

Hillary, F. G., & Grafman, J. H. (2017). Injured brains and adaptive networks: The benefits and costs of hyperconnectivity. *Trends in Cognitive Sciences*, *21*(5), 385–401. https://doi.org/10.1016/j.tics.2017.03.003

Huang, C.-Y., Chang, G.-C., Tsai, Y.-Y., & Hwang, I.-S. (2016). An increase in postural load facilitates an anterior shift of processing resources to frontal executive function in a postural-suprapostural task. *Frontiers in Human Neuroscience*, *10*(August), 420. https://doi.org/10.3389/fnhum.2016.00420

Huang, C.-Y., Lin, L. L., & Hwang, I.-S. (2017). Age-related differences in reorganization of functional connectivity for a dual task with increasing postural destabilization. *Frontiers in Aging Neuroscience*, *9*(April). https://doi.org/10.3389/fnagi.2017.00096

Imms, P., Clemente, A., Cook, M., D'Souza, W., Wilson, P. H., Jones, D. K., & Caeyenberghs, K. (2019). The structural connectome in traumatic brain injury: A meta-analysis of graph metrics. *Neuroscience & Biobehavioral Reviews*, *99*(April), 128–137. https://doi.org/10.1016/j.neubiorev.2019.01.002

Inglese, M., Makani, S., Johnson, G., Cohen, B. A., Silver, J. A., Gonen, O., & Grossman, R. I. (2005). Diffuse axonal injury in mild traumatic brain injury: A diffusion tensor imaging study. *Journal of Neurosurgery*, *103*(2), 298–303. https://doi.org/10.3171/jns.2005.103.2.0298

Kaufman, K. R., Brey, R. H., Chou, L.-S., Rabatin, A., Brown, A. W., & Basford, J. R. (2006). Comparison of subjective and objective measurements of balance disorders following traumatic brain injury. *Medical Engineering & Physics*, *28*(3), 234–239. https://doi.org/10.1016/j.medengphy.2005.05.005

Klimesch, W., Fellinger, R., & Freunberger, R. (2011). Alpha oscillations and early stages of visual encoding. *Frontiers in Psychology*, *2*, 118. https://doi.org/10.3389/fpsyg.2011.00118

Makeig, S., Bell, A. J., Jung, T.-P., & Sejnowski, T. J. (1996). Independent component analysis of electroencephalographic data. In *Advances in neural information processing systems* (Vol. 8, pp. 145–151). Cambridge, MA: MIT Press.

Maris, E., & Oostenveld, R. (2007). Nonparametric statistical testing of EEG- and MEG-data. *Journal of Neuroscience Methods*, *164*(1), 177–190. https://doi.org/10.1016/j.jneumeth.2007.03.024

Medaglia, J. D. (2017). Functional neuroimaging in traumatic brain injury: From nodes to networks. *Frontiers in Neurology*, *8*(August), 407. https://doi.org/10.3389/fneur.2017.00407

Michel, C. M., & Brunet, D. (2019). EEG source imaging: A practical review of the analysis steps. *Frontiers in Neurology*, *10*(April), 325. https://doi.org/10.3389/fneur.2019.00325

Mierau, A., Pester, B., Hülsdünker, T., Schiecke, K., Strüder, H. K., & Witte, H. (2017). Cortical correlates of human balance control. *Brain Topography*, *30*(4), 434–446. https://doi.org/10.1007/s10548-017-0567-x

Miraglia, F., Vecchio, F., & Rossini, P. M. (2018). Brain electroencephalographic segregation as a biomarker of learning. *Neural Networks*, *106*(October), 168–174. https://doi.org/10.1016/j.neunet.2018.07.005

Mullen, T., Kothe, C., Chi, M., Ojeda, A., Kerth, T., Makeig, S., … Cauwenberghs, G. (2015). Real-time neuroimaging and cognitive monitoring using wearable dry EEG. *IEEE Transactions on Biomedical Engineering*, *62*(11), 2553–2567. https://doi.org/10.1109/TBME.2015.2481482

Munia, T. T. K., Haider, A., Schneider, C., Romanick, M., & Fazel-Rezai, R. (2017). A novel EEG based spectral analysis of persistent brain function alteration in athletes with concussion history. *Scientific Reports*, *7*(1), 1–13. https://doi.org/10.1038/s41598-017-17414-x

Newman, M. E. J. (2006). Modularity and community structure in networks. *PNAS*, *99*(12), 7821–7826. https://doi.org/10.1073/pnas.122653799

Nordin, A. D., David Hairston, W., & Ferris, D. P. (2019). Human electrocortical dynamics while stepping over obstacles. *Scientific Reports*, *9*(1), 1–12. https://doi.org/10.1038/s41598-019-41131-2

Omlor, W., Patino, L., Mendez-Balbuena, I., Schulte-Monting, J., & Kristeva, R. (2011). Corticospinal beta-range coherence is highly dependent on the pre-stationary motor state. *Journal of Neuroscience*, *31*(22), 8037–8045. https://doi.org/10.1523/jneurosci.4153-10.2011

Oostenveld, R., & Oostendorp, T. F. (2002). Validating the boundary element method for forward and inverse EEG computations in the presence of a hole in the skull. *Human Brain Mapping*, *17*(3), 179–192. https://doi.org/10.1002/hbm.10061

OPhelan, K. H., Otoshi, C. K., Ernst, T., & Chang, L. (2018). Common patterns of regional brain injury detectable by diffusion tensor imaging in otherwise normal-appearing white matter in patients with early moderate to severe traumatic brain injury. *Journal of Neurotrauma*, *35*(5), 739–749. https://doi.org/10.1089/neu.2016.4944

O'Reilly, C., Lewis, J. D., & Elsabbagh, M. (2017). Is functional brain connectivity atypical in autism? A systematic review of EEG and MEG studies. *PLoS One*, *12*(5), e0175870. https://doi.org/10.1371/journal.pone.0175870

Owens, J. A., Spitz, G., Ponsford, J. L., Dymowski, A. R., & Willmott, C. (2018). An investigation of white matter integrity and attention deficits following traumatic brain injury. *Brain Injury*, *32*, 776–783. https://doi.org/10.1080/02699052.2018.1451656

Pascual-Marqui, R. D. (2002). Standardized low-resolution brain electromagnetic tomography (SLORETA): Technical details. *Methods and Findings in Experimental and Clinical Pharmacology*, *24*(Suppl D), 5–12.

Peterson, S. M., & Ferris, D. P. (2018). Differentiation in theta and beta electrocortical activity between visual and physical perturbations to walking and standing balance. *Eneuro*, *5*(4), ENEURO.0207–ENEU18.2018. https://doi.org/10.1523/eneuro.0207-18.2018

Peterson, S. M., & Ferris, D. P. (2019). Group-level cortical and muscular connectivity during perturbations to walking and standing balance. *NeuroImage*, *198*(September), 93–103. https://doi.org/10.1016/j.neuroimage.2019.05.038

Pickett, T. C. (2007). Objectively assessing balance deficits after TBI: Role of computerized posturography. *The Journal of Rehabilitation Research and Development*, *44*(7), 983–990. https://doi.org/10.1682/jrrd.2007.01.0001

Pilkar, R., Karunakaran, K. K., Veerubhotla, A., Ehrenberg, N., Ibironke, O., & Nolan, K. J. (2020). Evaluating sensory acuity as a marker of balance dysfunction after a traumatic brain injury: A psychophysical approach. *Frontiers in Neuroscience*, *14*(August). https://doi.org/10.3389/fnins.2020.00836

Pion-Tonachini, L., Kreutz-Delgado, K., & Makeig, S. (2019). ICLabel: An automated electroencephalographic independent component classifier, dataset, and website. *NeuroImage*, *198*(September), 181–197. https://doi.org/10.1016/J.NEUROIMAGE.2019.05.026

Rubinov, M., & Sporns, O. (2010). Complex network measures of brain connectivity: Uses and interpretations. *NeuroImage*, *52*(3), 1059–1069. https://doi.org/10.1016/j.neuroimage.2009.10.003

Salimi-Khorshidi, G., Smith, S. M., & Nichols, T. E. (2011). Adjusting the effect of nonstationarity in cluster-based and TFCE inference. *NeuroImage*, *54*, 2006–2019.

Scala, G., Di, M., Dupuy, E., Guillaud, E., Doat, E., Barse, B., ... Chanraud, S. (2019). Efficiency of sensorimotor networks: Posture and gait in young and older adults. *Experimental Aging Research*, *45*(1), 41–56. https://doi.org/10.1080/0361073x.2018.1560108

Schelter, B., Winterhalder, M., Eichler, M., Peifer, M., Hellwig, B., Guschlbauer, B., ... Timmer, J. (2006). Testing for directed influences among neural signals using partial directed coherence. *Journal of Neuroscience Methods*, *152*(1–2), 210–219. https://doi.org/10.1016/j.jneumeth.2005.09.001

Sharp, D. J., Scott, G., & Leech, R. (2014). Network dysfunction after traumatic brain injury. *Nature Reviews Neurology*, *10*(3), 156–166. https://doi.org/10.1038/nrneurol.2014.15

Shenton, M. E., Hamoda, H. M., Schneiderman, J. S., Bouix, S., Pasternak, O., Rathi, Y., ... Zafonte, R. (2012). A review of magnetic resonance imaging and diffusion tensor imaging findings in mild traumatic brain injury. *Brain Imaging and Behavior*, *6*(2), 137–192. https://doi.org/10.1007/s11682-012-9156-5

Slobounov, S. M., Teel, E., & Newell, K. M. (2013). Modulation of cortical activity in response to visually induced postural perturbation: Combined VR and EEG study. *Neuroscience Letters*, *547*, 6–9. https://doi.org/10.1016/j.neulet.2013.05.001

Slobounov, S., Wu, T., & Hallett, M. (2006). Neural basis subserving the detection of postural instability: An FMRI study. *Motor Control*, *10*(1), 69–89. https://doi.org/10.1123/mcj.10.1.69

Smith, L. G. F., Milliron, E., Ho, M.-L., Hu, H. H., Rusin, J., Leonard, J., & Sribnick, E. A. (2019). Advanced neuroimaging in traumatic brain injury: An overview. *Neurosurgical Focus*, *47*(6), E17. https://doi.org/10.3171/2019.9.focus19652

Smith, S. M., Jenkinson, M., Johansen-Berg, H., Rueckert, D., Nichols, T. E., Mackay, C. E., et al. (2006). Tract-based spatial statistics: Voxelwise analysis of multi-subject diffusion data. *NeuroImage*, *31*(4), 1487–1505. https://doi.org/10.1016/j.neuroimage.2006.02.024

Smith, S. M., Jenkinson, M., Woolrich, M. W., Beckmann, C. F., Behrens, T. E. J., Johansen-Berg, H., ... Matthews, P. M. (2004). Advances in functional and structural MR image analysis and implementation as FSL. *NeuroImage*, *23*(January), S208–S219. https://doi.org/10.1016/j.neuroimage.2004.07.051

Smith, S. M., Johansen-Berg, H., Jenkinson, M., Rueckert, D., Nichols, T. E., Miller, K. L., ... Behrens, T. E. J. (2007). Acquisition and voxelwise analysis of multi-subject diffusion data with tract-based spatial statistics. *Nature Protocols*, *2*(3), 499–503. https://doi.org/10.1038/nprot.2007.45

Solis-Escalante, T., van der Cruijsen, J., de Kam, D., van Kordelaar, J., Weerdesteyn, V., & Schouten, A. C. (2019). Cortical dynamics during preparation and execution of reactive balance responses with distinct postural demands. *NeuroImage*, *188*(September 2018), 557–571. https://doi.org/10.1016/j.neuroimage.2018.12.045

Sporns, O. (2013). Network attributes for segregation and integration in the human brain. *Current Opinion in Neurobiology*, *23*(2), 162–171. https://doi.org/10.1016/j.conb.2012.11.015

Stam, C. J. (2014). Modern network science of neurological disorders. *Nature Reviews Neuroscience*, *15*(10), 683–695. https://doi.org/10.1038/nrn3801

Surgent, O. J., Dadalko, O. I., Pickett, K. A., & Travers, B. G. (2019). Balance and the brain: A review of structural brain correlates of postural balance and balance training in humans. *Gait & Posture*, *71*, 245–252. https://doi.org/10.1016/j.gaitpost.2019.05.011

Tadel, F., Baillet, S., Mosher, J. C., Pantazis, D., & Leahy, R. M. (2011). Brainstorm: A user-friendly application for MEG/EEG analysis. *Computational Intelligence and Neuroscience*, *2011*, 1–13. https://doi.org/10.1155/2011/879716

Takakusaki, K. (2017). Functional neuroanatomy for posture and gait control. *Journal of Movement Disorders*, *10*(1), 1–17. https://doi.org/10.14802/jmd.16062

Talalay, I. V., Kurgansky, A. V., & Machinskaya, R. I. (2018). Alpha-band functional connectivity during cued versus implicit modality-specific anticipatory attention: EEG-source coherence analysis. *Psychophysiology*, *55*(12), e13269. https://doi.org/10.1111/psyp.13269

Taylor, C. A., Bell, J. M., Breiding, M. J., & Likang, X. (2017). Traumatic brain injury-related emergency department visits, hospitalizations, and deaths—United States, 2007 and 2013. *MMWR*, *66*(9), 1–16. https://doi.org/10.15585/mmwr.ss6609a1

Teasdale, G., & Jennett, B. (1974). Assessment of coma and impaired consciousness. A practical scale. *Lancet*, *2*, 81–84.

Uddin, M. N., Figley, T. D., Solar, K. G., Shatil, A. S., & Figley, C. R. (2019). Comparisons between multi-component myelin water fraction T1w/T2w ratio, and diffusion tensor imaging measures in healthy human brain structures. *Scientific Reports*, *9*(1), 2500. https://doi.org/10.1038/s41598-019-39199-x

van de Steen, F., Faes, L., Karahan, E., Songsiri, J., Valdes-Sosa, P. A., & Marinazzo, D. (2016). Critical comments on EEG sensor space dynamical connectivity analysis. *Brain Topography*, *32*(4), 643–654. https://doi.org/10.1007/s10548-016-0538-7

Varghese, J. P., Staines, W. R., & McIlroy, W. E. (2019). Activity in functional cortical networks temporally associated with postural instability. *Neuroscience*, *401*, 43–58. https://doi.org/10.1016/j.neuroscience.2019.01.008

Veeramuthu, V., Narayanan, V., Kuo, T. L., Delano-Wood, L., Chinna, K., Bondi, M. W., ... Ramli, N. (2015). Diffusion tensor imaging parameters in mild traumatic brain injury and its correlation with early neuropsychological impairment: A longitudinal study. *Journal of Neurotrauma*, *32*, 1497–1509. https://doi.org/10.1089/neu.2014.3750

Venkatesan, U. M., & Hillary, F. G. (2019). Functional connectivity within lateral posterior parietal cortex in moderate to severe traumatic brain injury. *Neuropsychology*, *33*(6), 893–910. https://doi.org/10.1037/neu0000553

Voelbel, G. T., Genova, H. M., Chiaravalloti, N. D., & Hoptman, M. J. (2012). Diffusion tensor imaging of traumatic brain injury review: Implications for neurorehabilitation. *NeuroRehabilitation*, *31*(3), 281–293. https://doi.org/10.3233/nre-2012-0796

Wallace, E. J., Mathias, J. L., & Ward, L. (2018). Diffusion tensor imaging changes following mild moderate and severe adult traumatic brain injury: A meta-analysis. *Brain Imaging and Behavior*, *12*(6), 1607–1621. https://doi.org/10.1007/s11682-018-9823-2

Wang, B., Zhang, M., Lingguo, B., Xu, L., Wang, W., & Li, Z. (2016). Posture-related changes in brain functional connectivity as assessed by wavelet phase coherence of NIRS signals in elderly subjects. *Behavioural Brain Research*, *312*, 238–245. https://doi.org/10.1016/j.bbr.2016.06.037

Wittenberg, E., Thompson, J., Nam, C. S., & Franz, J. R. (2017). Neuroimaging of human balance control: a systematic review. *Frontiers in Human Neuroscience*, *11*, 170. http://dx.doi.org/10.3389/fnhum.2017.00170.

Xia, M., Wang, J., & He, Y. (2013). BrainNet viewer: A network visualization tool for human brain connectomics. *PLoS One*, *8*(7), e68910. https://doi.org/10.1371/journal.pone.0068910

Yoncheva, Y. N., Somandepalli, K., Reiss, P. T., Kelly, C., di Martino, A., Lazar, M., … Xavier Castellanos, F. (2016). Mode of anisotropy reveals global diffusion alterations in attention-deficit/hyperactivity disorder. *Journal of the American Academy of Child & Adolescent Psychiatry*, *55*(2), 137–145. https://doi.org/10.1016/j.jaac.2015.11.011

Zhang, Y., Brady, M., & Smith, S. (2001). Segmentation of brain MR images through a hidden Markov random field model and the expectation-maximization algorithm. *IEEE Transactions on Medical Imaging*, *20*, 45–57.

Zhou, Y. (2017). Small world properties changes in mild traumatic brain injury. *Journal of Magnetic Resonance Imaging*, *46*(2), 518–527. https://doi.org/10.1002/jmri.25548

SUPPORTING INFORMATION

Additional supporting information may be found online in the Supporting Information section at the end of this article.